# DISCRETE TIME PROPAGATION GRAPHS FOR OPTICAL SCATTERING

PHILIP ETTER

*Advised by Professor Jason Fleischer*

Abstract. In this paper, we examine discrete time propagation graphs as a potential framework for thin scattering layer models. The particular class of interest are propagation graphs formed from Cayley graphs of $\mathbb{Z}^d$, as their underlying geometry and shift-invariance make them appealing as potential models of the desired physical process. We show that their shift-invariant nature makes it possible to use Fourier analysis and residue calculus to recover exact expressions for transfer functions on the graph when $d = 1$. Moreover, we reduce the propagation of Fourier modes on the graph in the general case to the $d = 1$ case, and provide exact solutions for propagation in a layer of the graph with a finite depth. We also consider direction-dependent propagation (e.g. Mie scattering) and extend both the models and methods developed to this new regime. The mathematical tools developed in this paper may provide a framework for the future development of a model of thin scattering layers using graph theory.

## 1. Introduction

Thin scattering layers exhibit a property known as the *memory effect*, whereby a shift by a small angle $\Delta\theta$ to the incidence angle of an ingoing optical pulse will produce a corresponding shift $\Delta x$ to the speckle pattern produced on the other side of the layer. Within a sufficiently small region, this effect can be used to recover the autocorrelation of an input signal from a measured output signal [1, 2], allowing one to image through these layers by exploiting their statistical properties. Our goal is to study the scattering of light through thin layers from a different perspective. We aspire to produce a graph theoretical model of light scattering through thin scattering layers, with the hope that such a model may shed new light on the memory effect.

As the theoretical framework for our model, we consider a time-discretized variety of the propagation graph structure found in the engineering literature (see [3]). These graphs describe the linear propagation of an input signal through an arbitrary network structure. Given such a finite propagation graph, transfer functions between individual nodes can be computed via means of the resolvent (the "transfer matrix") of the edge matrix between vertices in the network. We are particularly interested in propagation on grid-like structures, where every vertex corresponds to a position in space, and where the graph exhibits some kind of self-similarity. Therefore, we extend the theory of propagation graphs to a number of special infinite graphs, particularly Cayley graphs of $\mathbb{Z}^d$, as well as special directed versions thereof. We consider what happens when propagation is restricted only to a thin layer of these graphs, and develop methods for computing exact transfer functions from one side of the layer to the other.

Unfortunately, direct computation of the resolvent via matrix inversion is not always possible – the graph may be infinite for example, as will commonly be the case in this paper. But in the cases of interest to us, there are analytic techniques by which one can write down the entries of the resolvent. While computation of arbitrary entries of the resolvent is usually not possible, we have developed a number of algebraic techniques which allow other entries of the resolvent to be recovered from knowledge of only a single entry or a knowledge of a few entries, which can be first computed using residue calculus.

*Date*: June 14, 2017.

The project was funded in part by the Princeton mathematics department.

This paper is structured primarily in three parts. In the first, we give a brief overview of propagation graphs. We then transition to propagation on Cayley graphs of $\mathbb{Z}^d$ and within thin layers of these graphs. Finally, we extend the theory to the case where incidence direction determines the manner in which a signal continues to propagate (e.g. Mie scattering). We also consider propagation graph models where the underlying graph structure or the transfer functions on the edges are random. A discussion of these models can be found in appendix A.

## 2. Propagation Graphs

A propagation graph is a model of linear time-invariant propagation of a signal through a directed network. A signal introduced to a vertex in the graph will propagate along the outgoing edges of that vertex to other vertices in the graph. When this happens, each edge alters the incoming signal by applying a transfer function. The destination vertex of the edge then receives this modified signal. In the case where a vertex receives multiple signals from its ingoing edges, they are simply added linearly. The signal then continues to propagate ad infinitum in the same manner. Since the propagation of the signal through this graph is both linear and time-invariant, we can consider transfer functions between individual vertices in the graph.

### 2.1. **Discrete Time.**

The signals in question may be either discrete or continuous. We will differentiate between the two by using brackets for discrete signals $f[t]$, and parenthesis for continuous signals $f(t)$. For discrete time, relevant transfer functions are in terms of the z-transform, defined as

$$F(z) \equiv \mathcal{Z}[f] = \sum_{t=-\infty}^{\infty} f[t] z^{-t} \,. \tag{2.1}$$

To define discrete-time propagation graphs, we now proceed as follows: Let $G = (V, E)$ be a directed graph and for each edge $(i, j) \in E$, let $\Omega_{ij}(z)$ be the transfer function of edge $(i, j)$. Propagation can now be formulated using these transfer functions. Each vertex $i \in V$ has a corresponding signal $\psi_i[t]$ with z-transform $\Psi_i(z) = \mathcal{Z}[\psi_i]$. These signals are related by the propagation equation

$$\Psi_j(z) = \sum_{(i,j)\in E} \Omega_{ij}(z)\Psi_i(z) \,. \tag{2.2}$$

As we can see, the z-transform of a signal $\Psi_j$ is the sum of all the signals on incoming edges $(i, j)$, modulated by the respective transfer functions $\Omega_{ij}$. However, the propagation equation (2.2) is sourceless, it does not allow us to introduce signals into the graph. To introduce a signal $\phi_j[t]$ at vertex $j$, we add the z-transform $\Phi_j(z) = \mathcal{Z}[\phi_j]$ to the propagation equation above, i.e.

$$\Psi_j(z) = \sum_{(i,j)\in E} \Omega_{ij}(z)\Psi_i(z) + \Phi_j(z) \,. \tag{2.3}$$

The *edge matrix* $T(z)$ is defined using the transfer functions of the edges,

$$T_{ij}(z) \equiv \begin{cases} \Omega_{ji}(z) & : (i, j) \in E \\ 0 & : \text{o.w.} \end{cases} \,. \tag{2.4}$$

Using this matrix, we can rewrite (2.3) in matrix form,

$$\vec{\Psi}(z) = T(z)\vec{\Psi}(z) + \vec{\Phi}(z) \,. \tag{2.5}$$

We can solve for $\vec{\Psi}(z)$:

$$\vec{\Psi}(z) = (I - T(z))^{-1}\vec{\Phi}(z) \tag{2.6}$$

We will call the operator $M(z) \equiv (I - T(z))^{-1}$ the *transfer matrix* of the system. The entries of $M(z)$ are the transfer functions between individual vertices. Note that if a lone signal with z-transform $\Phi_i(z)$ is introduced at a vertex $i$, then (2.6) results in

$$\Psi_j(z) = M_{ji}(z)\Phi_i(z) \,. \tag{2.7}$$

In our upcoming analyzes, it is also useful to consider a power expansion of the operator $M(z)$. The operator $M(z)$ can be expressed in terms of the Neumann series,

$$(I - T(z))^{-1} \sim \sum_{n=0}^{\infty} T(z)^n \,. \tag{2.8}$$

This expansion holds when $|z|$ is large enough such that the right hand of the equation converges in the operator norm. Before we proceed, let us illustrate how the above generalizes to continuous time.

2.2. **Continuous Time.** For continuous time, the transfer functions $\Omega_{ij}$ are with respect to the Laplace transform,

$$F(s) \equiv \mathcal{L}[f] = \int_0^{\infty} f(t) e^{-st} \, dt \,. \tag{2.9}$$

All of the definitions are essentially the same as with the discrete time case. The propagation equation becomes

$$\Psi_j(s) = \sum_{(i,j)\in E} \Omega_{ij}(s)\Psi_i(s) + \Phi_j(s) \,, \tag{2.10}$$

where $\Psi_i(s) = \mathcal{L}[\psi_i]$ and $\Phi_i(s) = \mathcal{L}[\phi_i]$. Furthermore, both (2.6) and (2.8) carry over into the continuous time case. Though we will not use it, the continuous time case allows us finer control over time delays. Alternatively, we could use the Fourier transform instead of the Laplace transform. However, the Laplace transform has the advantage that it can handle systems which may highly unstable. Propagation graphs of this form are the ones conventionally used in the engineering literature.

2.3. **Relationship to Matrix Spectra.** The transfer matrix from (2.6) is closely related to the spectrum of the operator $T(z)$ at a given $z \in \mathbb{C}$. For example, suppose that $T(z)$ has a spectral decomposition

$$T(z) = \Lambda(z) \left[ \bigoplus_i \lambda_i(z) \right] \Lambda(z)^\dagger \,, \tag{2.11}$$

where $\Lambda(z)$ is unitary and $\lambda_i(z)$ are the real eigenvalues of $T(z)$. It is easy to see that the transfer matrix $M(z) \equiv (I - T(z))^{-1}$ is then given by

$$M(z) = \Lambda(z) \left[ \bigoplus_i \frac{1}{1 - \lambda_i(z)} \right] \Lambda(z)^\dagger \,. \tag{2.12}$$

From the above equation and the fact that

$$\det(I - T(z)) = \prod_i (1 - \lambda_i(z)) \,, \tag{2.13}$$

we see that the poles of the transfer functions occur where $\lambda_i(z) = 1$. Moreover, this also holds for matrices that do not necessarily have such a spectral decomposition. The placement of these poles gives us an idea of behavior and stability of the corresponding impulse response. In particular, the locations of these poles allows determines whether the resulting system is stable.

Perhaps the simplest systems we can analyze are those with unit delay, that is, where the edge transfer matrix takes the form

$$T(z) = z^{-1} A \tag{2.14}$$

for some matrix $A$. Such a form means that each edge delays its input by 1 unit of time and modulates it by a factor of $A_{ij}$. For these type of matrices, we simply have $\lambda_i(z) = z^{-1}\lambda_i$ where $\lambda_i$

denote the eigenvalues of $A$. Therefore, the poles of the transfer functions for these type of systems occur precisely where $z = \lambda_i$. Indeed, (2.12) simply becomes

$$M(z) = \Lambda \left[ \bigoplus_i \frac{1}{1 - z^{-1}\lambda_i} \right] \Lambda^\dagger \,. \tag{2.15}$$

## 3. Signal Propagation on Cayley Graphs of $\mathbb{Z}^n$

Our original project goal was to construct a graph-theoretical model of thin scattering layers by taking the underlying graph to be random, i.e. taking $A$ to be a random matrix selected from some ensemble. Appendix A describes some of the models we examined and analyzed during the course of this project. However, as one might expect, randomness seems to be insufficient to produce meaningful physical models. Indeed, without extra considerations, it is difficult to identify such a model with the propagation of light through a thin scattering layer. While such models account for random structure, they are flawed because they lack a solid notion of the underlying geometry. Therefore, we turn to studying propagation on Cayley graphs of $\mathbb{Z}^d$. These graphs generalize the notion of propagation on a grid in $d$-dimensions, and as we will show, in certain scenarios it is possible to compute closed-form solutions using analytic techniques. Our hope is that the mathematical models we present in this paper can be further modified to produce a model of thin scattering layers which coincides with experiment. The mathematical techniques we present in this paper may then be used to analyze such a model.

The choice of Cayley graphs of $\mathbb{Z}^d$ is motivated primarily by mathematical and geometrical concerns. As already mentioned, these graphs generalize a notion of geometry we are looking for. Furthermore, they also posses a notion of shift-invariance. Shift-invariance is particularly important because it makes the computation of transfer functions tractable in some situations. While at first such a restriction may seem overbearing, we believe it is reasonable to assume some notion of shift-invariance given the problem we are trying to model. The small-scale structure of a scattering layer may not be invariant under translations, but the underlying character of the random structure is. Hence, building shift-invariance into our model both makes physical sense and is also helpful from a mathematical perspective, because it means we can apply tools from Fourier analysis.

We endeavor to develop a shift-invariant model together with rudimentary tools to extract useful information from the result. The first natural step in this direction is to consider graphs which look approximately like "grids." The idea is that each vertex of these graph corresponds a scattering site, where some scattering event occurs. Hence, these graph structures lend a notion of locality to the model which was previously missing.

We use Cayley graphs of $\mathbb{Z}^d$ as our generalization of "grid-like" graphs.[1] While these graphs are infinite, they benefit from an aforementioned notion of locality and distance. An example graph can be seen in figure 1. Consider such a Cayley graph $G$ of $\mathbb{Z}^d$ with generators $\{\boldsymbol{g}_1, \boldsymbol{g}_2, ..., \boldsymbol{g}_k\}$. To convert this graph into a propagation graph, we associate with each generator $\boldsymbol{g} \in \mathcal{G}$ a corresponding transfer function $\Omega_{\boldsymbol{g}}(z)$, with the understanding that when the signal traverses an edge corresponding to $\boldsymbol{g}$, it picks up a factor of $\Omega_{\boldsymbol{g}}(z)$. Since we have made the transition from finite graphs to infinite graphs, the *edge matrix* $T(z)$ and the *transfer matrix* $M(z) = (I - T(z))^{-1}$ are no longer finite dimensional operators. Therefore, we instead frame propagation on the graph $G$ in terms of a propagation kernel in Fourier space. This propagation kernel is given by

$$K(\boldsymbol{\xi}; z) \equiv \sum_{\boldsymbol{g} \in \mathcal{G}} \Omega_{\boldsymbol{g}}(z)\, e^{2\pi i \boldsymbol{g}\cdot\boldsymbol{\xi}} \,, \tag{3.1}$$

where $\boldsymbol{\xi} = (\xi_1, \xi_2, ..., \xi_d)$ are the Fourier variables corresponding to the dual of the group $\mathbb{Z}^d$. To see how the kernel encodes propagation on the Cayley graph, consider the signals $\psi_v[t]$ at vertices

[1] Alternatively, one could also consider Cayley graphs of $\mathbb{Z}/m_1\mathbb{Z} \times \mathbb{Z}/m_2\mathbb{Z} \times ... \times \mathbb{Z}/m_d\mathbb{Z}$ instead. This corresponds to the finite periodic version of the infinite Cayley graphs of $\mathbb{Z}$. However, the analysis is easier to perform for infinite graphs than for finite ones because it allows for the use of tools from mathematical analysis.

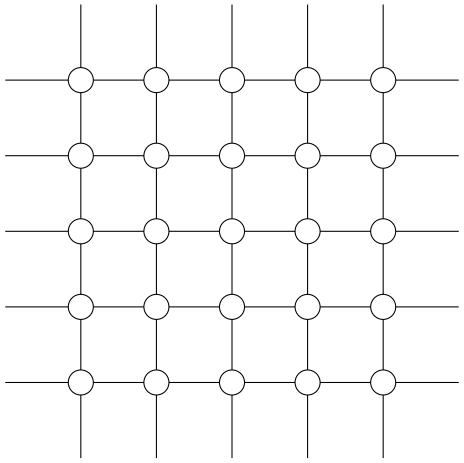

FIGURE 1. A section of the Cayley graph of $\mathbb{Z}^2$ with the generators $(1,0)$, $(0,1)$, $(-1,0)$, and $(0,-1)$. This graph is precisely an infinite two-dimensional grid graph. This graph is the de facto example for all of the tools we develop in this section.

$\boldsymbol{v} = (v_1, v_2, ..., v_d)$. The underlying system is governed by the equations

$$\vec{\Psi}(z) = T(z)\vec{\Psi}(z) + \vec{\Phi}(z)\,, \tag{3.2}$$

where $\Psi_{\boldsymbol{v}} = \mathcal{Z}[\psi_{\boldsymbol{v}}]$, $\Phi_{\boldsymbol{v}}(z)$ is the input to the system at vertex $v$, and $T(z)$ is the transfer matrix defined as in equation (2.4). Since we are on a Cayley graph, $T(z)$ has a simple form. Writing equation (3.2) in terms of the individual entries gives

$$\Psi_{\boldsymbol{v}}(z) = \sum_{\boldsymbol{g}\in\mathcal{G}} \Omega_{\boldsymbol{g}}(z)\Psi_{\boldsymbol{v}-\boldsymbol{g}}(z) + \Phi_{\boldsymbol{v}}(z)\,. \tag{3.3}$$

We define the spatial Fourier transform $\hat{\Psi}$ as

$$\hat{\Psi}(\boldsymbol{\xi}; z) \equiv \sum_{\boldsymbol{v}\in\mathbb{Z}^d} e^{-2\pi i\boldsymbol{\xi}\cdot\boldsymbol{v}}\, \Psi_{\boldsymbol{v}}(z)\,, \tag{3.4}$$

and likewise for $\hat{\Phi}$. The inverse of definition (3.4) is given by the Fourier inversion formula,

$$\Psi_{\boldsymbol{v}}(z) = \int_{-1/2}^{1/2} e^{2\pi i\boldsymbol{\xi}\cdot\boldsymbol{v}}\, \hat{\Psi}(\boldsymbol{\xi}; z)\, d\boldsymbol{\xi}\,. \tag{3.5}$$

Taking the spatial Fourier transform of equation (3.3) now gives us

$$\hat{\Psi}(\boldsymbol{\xi}; z) = \sum_{\boldsymbol{g}\in\mathcal{G}} \Omega_{\boldsymbol{g}}(z)\, e^{2\pi i\boldsymbol{g}\cdot\boldsymbol{\xi}}\, \hat{\Psi}(\boldsymbol{\xi}; z) + \hat{\Phi}(\boldsymbol{\xi}; z)\,, \tag{3.6}$$

which we immediately recognize as

$$\hat{\Psi}(\boldsymbol{\xi}; z) = K(\boldsymbol{\xi}; z)\, \hat{\Psi}(\boldsymbol{\xi}; z) + \hat{\Phi}(\boldsymbol{\xi}; z)\,. \tag{3.7}$$

From this, we may solve for the desired quantity $\hat{\Psi}$,

$$\hat{\Psi}(\boldsymbol{\xi}; z) = \frac{1}{1 - K(\boldsymbol{\xi}; z)}\hat{\Phi}(\boldsymbol{\xi}; z)\,. \tag{3.8}$$

Inverting the Fourier transform,

$$\Psi_{\boldsymbol{v}}(z) = \int_{-1/2}^{1/2} \frac{e^{2\pi i\boldsymbol{\xi}\cdot\boldsymbol{v}}}{1 - K(\boldsymbol{\xi}; z)}\hat{\Phi}(\boldsymbol{\xi}; z)\, d\boldsymbol{\xi} = \sum_{\boldsymbol{w}\in\mathbb{Z}^d} \left[\int_{-1/2}^{1/2} \frac{e^{2\pi i\boldsymbol{\xi}\cdot(\boldsymbol{v}-\boldsymbol{w})}}{1 - K(\boldsymbol{\xi}; z)}\, d\boldsymbol{\xi}\right] \Phi_{\boldsymbol{w}}(z)\,. \tag{3.9}$$

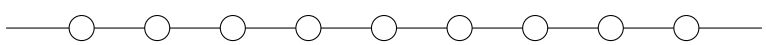

FIGURE 2. A section of the Cayley graph of $\mathbb{Z}$ with the generators 1 and $-1$.

Hence, in this scenario, the transfer matrix $M(z)$ has entries given by

$$M_{\boldsymbol{vw}}(z) = \int_{-1/2}^{1/2} \frac{e^{2\pi i \boldsymbol{\xi}\cdot(\boldsymbol{v}-\boldsymbol{w})}}{1-K(\boldsymbol{\xi};z)}\, d\boldsymbol{\xi} \tag{3.10}$$

The impulse response from one vertex to any other vertex can now be computed by extracting the $z^{-t}$ coefficients of the above expression using the inverse z-transform. Note that eq. (3.10) depends only on the difference between the two vertices $\boldsymbol{v}$ and $\boldsymbol{w}$, as one would expect from a shift-invariant system. Moreover, eq. (3.10) encodes all of the propagation information of the entire system. But while the transfer matrix (3.10) is a nice expression, computing it in closed form for all $\boldsymbol{v}$ and $\boldsymbol{w}$ can prove difficult.

As an example, we consider the probability distribution of a random walk on $G$. For a simple random walk, we set

$$\Omega_{\boldsymbol{g}}(z) \equiv \frac{z^{-1}}{k}\,. \tag{3.11}$$

For a random walk on a grid graph of dimension $d$, where the generators are given by $\pm\delta_1$, $\pm\delta_2$, ..., $\pm\delta_d$, the propagator becomes

$$K(\boldsymbol{\xi};z) = \frac{z^{-1}}{d}\sum_{j=1}^{d}\cos 2\pi\xi_j\,. \tag{3.12}$$

The corresponding transfer matrix entries are given by eq. (3.10). These are difficult to compute generally, but we can oftentimes compute them when $\boldsymbol{v}=\boldsymbol{w}$. For example, as we will see shortly, in the case where $d=1$, for $|z|>1$,

$$M_{\boldsymbol{vv}}(z) = \frac{1}{\sqrt{1-z^{-2}}} = 1+\frac{1}{2}z^{-2}+\frac{3}{8}z^{-4}+\frac{5}{16}z^{-6}+O(z^{-8}) = \sum_{n=0}^{\infty}\frac{1}{2^{2n}}\binom{2n}{n}z^{-2n}\,. \tag{3.13}$$

Note that the coefficients of $z^{-t}$ correspond to the probabilities that the random walk lands on vertex $\boldsymbol{v}$ after $t$ time steps.

3.1. **The Special Case of Symmetric Grid Graphs in Dimension One.** In general, analysis of the transfer matrix $M(z)$ entries via the formulation in eq. (3.10) can be very difficult. However, there is one case where the analysis is significantly easier – the case in which $G$ is an undirected path in dimension one. Here, the generators of $G$ in $\mathbb{Z}$ are given by $g_1=1$ and $g_2=-1$ and the result is a graph which resembles an infinite chain, as seen in figure 2. Moreover, we suppose that the propagation is symmetric, that is,

$$\Omega_1(z) = \Omega_{-1}(z) \tag{3.14}$$

In this case, we simply call the transfer function above $\Omega(z)$ and assume that all edges have transfer function $\Omega(z)$. Physically, this means that there is no distinction between the signal scattering from the left or the right. To begin the analysis, we want to know what we call the *self-transfer function* $S(z)\equiv M_{vv}(z)$. We note that eq. (3.10) gives us an analytic expression for $S(z)$,

$$S(z) = \int_{-1/2}^{1/2}\frac{1}{1-K(\xi;z)}\,d\xi\,. \tag{3.15}$$

Noting that $K(\xi;z)$ is 1-periodic in $\xi$, we can evaluate $S(z)$ using complex analysis by shifting the contour. In general, $K(\xi;z)$ can be made exponentially large by taking $\xi$ with large imaginary

component. This means by taking the contour

$$\gamma_R : -1/2 \to 1/2 \to 1/2 + iR \to -1/2 + iR \to -1/2\,, \tag{3.16}$$

residue calculus gives us

$$\oint_{\gamma_R} \frac{1}{1 - K(\xi; z)}\, d\xi = 2\pi i \sum_{\xi_k} \mathrm{res}_{\xi \to \xi_k} \frac{1}{1 - K(\xi; z)}\,, \tag{3.17}$$

where the sum is over all zeroes of $1 - K(\xi_k; z)$ in the interior of $\gamma_R$ when $|z| > 1$. Moreover, note that the vertical parts of the contour integral cancel since $K(\xi; z)$ is 1-periodic in $\xi$. As we take $R \to \infty$, $K(\xi; z)$ becomes very large, so the integral over the lower part of the contour vanishes, leaving us with

$$S(z) = \lim_{R\to\infty} \oint_{\gamma_R} \frac{1}{1 - K(\xi; z)}\, d\xi = 2\pi i \sum_{\xi_k} \mathrm{res}_{\xi \to \xi_k} \frac{1}{1 - K(\xi; z)}\,, \tag{3.18}$$

where the sum is now over all zeroes of $1 - K(\xi, z)$ with $-1/2 < \mathrm{Re}[\xi] < 1/2$ and $\mathrm{Im}[\xi] > 0$.

For illustrative purposes, we'll compute the self-transfer function using this method for a simple random walk on $\mathbb{Z}$. To make the notation simpler, we will use $\omega \equiv z^{-1}$. As per eq. (3.12), we have

$$K(\xi; \omega) = \omega \cos 2\pi\xi\,. \tag{3.19}$$

The only relevant zero of $1 - K(\xi; \omega)$ now occurs at $\xi_0 = \frac{1}{2\pi} \cos^{-1} \frac{1}{\omega}$. The residue at this point can be computed to be

$$\mathrm{res}_{\xi \to \xi_0} \frac{1}{1 - \omega \cos 2\pi\xi} = -\frac{1}{2\pi\sqrt{\omega^2 - 1}}\,. \tag{3.20}$$

eq. (3.17) now gives us the correct result for $S(z)$,

$$S(z) = \frac{1}{\sqrt{1 - z^{-2}}} \tag{3.21}$$

This brings us part of the way to finding the desired result $M_{vw}(z)$ for arbitrary $v$ and $w$. The second step in deriving the full transfer matrix $M(z)$ is a clever use of the symmetry of the system. Let $N(z)$ denote the transfer function of a vertex to its neighbor, that is $N(z) = M_{v+1,v}(z)$. By symmetry, we must also have $N(z) = M_{v-1,v}(z)$, since both the vertex to the left of $v$ and the vertex to the right of $v$ will have the same transfer function from $v$. First, we use the identity

$$M(z) = T(z)M(z) + I\,. \tag{3.22}$$

Taking the $vv$-entry of this matrix equation gives

$$M_{vv}(z) = \sum_w T_{vw}(z) M_{wv}(z) + I\,. \tag{3.23}$$

But since $T_{vw}(z) = 0$ except when $w = v \pm 1$, where it equals $\Omega(z)$, we get

$$S(z) = 2\Omega(z)N(z) + 1\,, \tag{3.24}$$

and correspondingly,

$$N(z) = \frac{S(z) - 1}{2\Omega(z)}\,. \tag{3.25}$$

Note that the same trick to derive the neighbor transfer function $N(z)$ can be done in any number of dimensions where the $\Omega_i(z)$ are all equal. As we will see, in higher dimensions it is difficult to go further than an immediate neighbor. However, the one dimensional case is special because in order to traverse the graph from one vertex to another, it is necessary that one visit all the vertices in between. This feature gives rise to a clever trick which will allow us to go beyond immediate neighbors and derive a full closed-form solution. But first, we must introduce some new machinery.

3.2. **Sinks and Marked Vertices.** Eventually, we want to be able to designate areas of the grid as "sinks" such that any signal entering these areas will be removed from the system, corresponding to the notion of light leaving a scattering layer. But first, let us try to break the transfer functions in the matrix $M(z)$ up into components based on how many times the signal hits a certain vertex $v$. To do this, we add a dummy variable $x$ to the transfer function each time a specific vertex $v$ is touched. As such, we rewrite the governing equations as

$$\vec{\Psi}(z,x) = [I + (x-1)P_v]\, T(z)\vec{\Psi}(z,x) + \vec{\Phi}(z)\,, \tag{3.26}$$

where $P_v = \delta_v \delta_v^\dagger$ is the projection operator onto vertex $v$. This adds a factor of the dummy variable $x$ to the incoming edges of the vertex $v$. The transfer matrix now becomes

$$M(z,x) = \left[I - [I + (x-1)P_v]\, T(z)\right]^{-1}\,. \tag{3.27}$$

The resulting signal is naturally split up into components where the $n$th component corresponds to the part of the signal which passes through the vertex $v$ $n$ times,

$$\vec{\Psi}(z,x) = M(z,x)\vec{\Phi}(z) = \sum_{j=0}^{\infty} \vec{\Psi}^{(j)}(z)\, x^j\,. \tag{3.28}$$

Note that the above corresponds to a Taylor expansion in $x$. Hence, each component can be calculated via the equation

$$\vec{\Psi}^{(n)}(z) = \frac{1}{n!}\frac{\partial^n}{\partial x^n}\vec{\Psi}(z,0) \tag{3.29}$$

With a little more effort, we can mark multiple vertices $v_1, v_2, ..., v_m$ at once by simply rewriting the governing equations again:

$$\vec{\Psi}(z,x_1,...,x_m) = \left[I + \sum_{i=1}^{m}(x_i-1)P_{v_i}\right] T(z)\vec{\Psi}(z,x_1,...,x_m) + \vec{\Phi}(z)\,. \tag{3.30}$$

The signal is now split via the dummy variables $x_i$, and the component of the signal with coefficient $x_1^{j_1}x_2^{j_2}...x_m^{j_m}$ corresponds to the part of the signal which has passed $j_1$ times through vertex $x_1$, $j_2$ times through vertex $x_2$ , etc. We obtain similar expressions for the multi-vertex case:

$$\begin{aligned} M(z,x_1,x_2,...,x_m) &= \left[I - \left[I + \sum_{i=1}^{m}(x_i-1)P_{v_i}\right] T(z)\right]^{-1}\,, \\ \vec{\Psi}(z,x_1,x_2,...,x_m) &= \sum_{j_1,j_2,...,j_m=0}^{\infty} \vec{\Psi}^{(j_1,j_2,...,j_m)}(z)\, x_1^{j_1}x_2^{j_2}...x_m^{j_m}\,, \\ \vec{\Psi}^{(n_1,n_2,...,n_m)}(z) &= \frac{1}{n_1!\,n_2!\,...\,n_m!}\frac{\partial^{n_1}}{\partial x_1^{n_1}}\frac{\partial^{n_2}}{\partial x_2^{n_2}}...\frac{\partial^{n_m}}{\partial x_m^{n_m}}\vec{\Psi}(z,0,0,...,0)\,. \end{aligned} \tag{3.31}$$

If we set $x_1 = x_2 = ... = x_m = 0$, then the vertices $x_1, x_2, ..., x_m$ are what we will call "sinks," as they essentially absorb any incoming signal. The result is equivalent to removing the vertices corresponding to markers $x_1, ..., x_m$ from the system entirely. On the other hand, if we set $x_1 = x_2 = ... = x_m = 1$, then we recover the original system. Indeed, one can think of the factors $x_i$ as attenuation to any signals entering the vertices $v_i$.

The natural question is to ask how this change of equations modifies the transfer matrix $M$. First, for the sake of clean notation, we define

$$A(z,x_1,x_2,...,x_m) = \sum_{i=1}^{m}(x_i-1)P_{v_i}\,. \tag{3.32}$$

To further condense notation, we write $x$ instead of $x_1, x_2, ..., x_m$. Let the new transfer matrix obtained from introducing these sinks be denoted by $M(z,x)$ and the old transfer matrix be denoted

by $M(z) = M(z,1)$. We use the shorthand,

$$J(z,x) = M(z,x) - I\,, \tag{3.33}$$

and correspondingly $J(z) = J(z,1)$. From the above eq. (3.32), we can write

$$J(z,x) = [I - (I + A(x))T(z)]^{-1} - I = \sum_{n=1}^{\infty} [(I + A(x))T(z)]^n\,. \tag{3.34}$$

Now, we group the terms by how many times $T(z)$ appears before the first $A(x)$,

$$\begin{aligned}
J(z,x) &= \sum_{n=1}^{\infty} \left[ \sum_{j=1}^{n} [(I + A(x))T(z)]^{n-j} A(x) T(z)^j + T(z)^n \right] \\
&= \sum_{j \le n} [(I + A(x))T(z)]^{n-j} A(x) T(z)^j + \sum_{n=1}^{\infty} T(z)^n \\
&= \sum_{j=1}^{\infty} \sum_{n=j}^{\infty} [(I + A(x))T(z)]^{n-j} A(x) T(z)^j + J(z) \\
&= \sum_{j=1}^{\infty} \sum_{n=0}^{\infty} [(I + A(x))T(z)]^{n} A(x) T(z)^j + J(z) \\
&= \sum_{j=1}^{\infty} M(z,x) A(x) T(z)^j + J(z) \\
&= (J(z,x) + I) A(x) \sum_{j=1}^{\infty} T(z)^j + J(z) \\
&= (J(z,x) + I) A(x) J(z) + J(z)\,.
\end{aligned} \tag{3.35}$$

Therefore, it follows that

$$J(z,x) = (A(x)J(z) + J(z))(I - A(x)J(z))^{-1}\,. \tag{3.36}$$

The above equation can be expanded into

$$J(z,x) = J(z) + A(x)J(z) + J(z)A(x)J(z) + A(x)J(z)A(x)J(z) + J(z)A(x)J(z)A(x)J(z)... \tag{3.37}$$

which is equivalent to

$$M(z,x) = M(z) + M(z)A(x)J(z) + M(z)A(x)J(z)A(x)J(z) + ... \tag{3.38}$$

Alternatively, we may write

$$M(z,x) = M(z)(I - A(x)J(z))^{-1}\,. \tag{3.39}$$

Note that all of the above derivations hold true for arbitrary $A(x)$. This provides a nice expression for the transfer function of the system with the vertices marked by $x_1, ..., x_m$ removed,

$$M(z,0) = M(z) \left[ I + \sum_{i=1}^{m} P_{v_i} J(z) \right]^{-1}\,. \tag{3.40}$$

In many cases, this expression is far more practical than deriving the transfer function of a system with a number of vertices removed outright. For example, considering the case of an infinite grid where there is an abundant amount of symmetry, it is already difficult enough to derive $M(z)$ in closed form. Removing a number of the vertices of the grid makes the problem of finding $M(z)$ even more difficult, since one can no longer rely on Fourier analysis if the symmetry of the grid is broken. Therefore, eq. (3.40) provides a nice alternative. Moreover, if the attenuation factor $1 - x$ is small, then it is possible to approximate $M(z,x)$ by truncating the series expansion (3.38).

FIGURE 3. Example propagation graph used for illustration. Gray vertex denotes a sink. When a signal enters this vertex it is absorbed (a signal may exit the vertex, however). The edge is given the transfer function $z^{-1}$.

For illustrative purposes, we provide a quick derivation of the above quantities for the graph shown in figure 3. The edge matrix $T(z)$ for this graph is given by

$$T(z) = \begin{bmatrix} 0 & z^{-1} \\ z^{-1} & 0 \end{bmatrix} . \tag{3.41}$$

An easy computation gives the unmodified transfer matrix where the sink vertex is treated as normal:

$$M(z) = \frac{1}{1-z^{-2}} \begin{bmatrix} 1 & z^{-1} \\ z^{-1} & 1 \end{bmatrix} = \begin{bmatrix} 1+z^{-2}+z^{-4}+... & z^{-1}+z^{-3}+z^{-5}+... \\ z^{-1}+z^{-3}+z^{-5}+... & 1+z^{-2}+z^{-4}+... \end{bmatrix} . \tag{3.42}$$

This transfer matrix is reasonable. Without any absorption of the signal at the left vertex in figure 1, whatever enters the system simply bounces back and forth between the two vertices forever. Treating the left vertex as a marked vertex gives us a modified transfer matrix which can be computed from eq. (3.39),

$$\begin{aligned} M(z,x) &= \frac{1}{1-xz^{-2}} \begin{bmatrix} 1 & xz^{-1} \\ z^{-1} & 1 \end{bmatrix} \\ &= \begin{bmatrix} 1+xz^{-2}+x^2z^{-4}+... & xz^{-1}+x^2z^{-3}+x^3z^{-5}+... \\ z^{-1}+xz^{-3}+x^2z^{-5}+... & 1+xz^{-2}+x^2z^{-4}+... \end{bmatrix} . \end{aligned} \tag{3.43}$$

If we make the vertex into a sink by setting $x = 0$, then we get

$$M(z,0) = \begin{bmatrix} 1 & 0 \\ z^{-1} & 1 \end{bmatrix} . \tag{3.44}$$

As we can see, this matrix corresponds to a system where signals may travel out of the left vertex, but anything entering the left vertex vanishes.

If we want to get a snapshot of what enters a given sink before it vanishes, we can examine expansions of the matrix $M(z, x_1, ..., x_m)$ in the variables $x_i$. In analogy to eq. (3.29), one has the expansion

$$M(z,x) = \sum_{i_1 i_2,...,i_m=0}^{\infty} M^{(i_1 i_2 ... i_m)}(z)\, x_1^{i_1} x_2^{i_2} ... x_m^{i_m} , \tag{3.45}$$

where $M^{(i_1 i_2 ... i_m)}(z)$ is the portion of the transfer matrix $M(z)$ that corresponds to paths entering the vertex $v_1$ a total of $i_1$ times, the vertex $v_2$ a total of $i_2$ times, etc. To get a snapshot of what enters a sink before vanishing, we simply need to consider the matrices $M^{(0...1...0)}(z)$, which can be extracted very easily from the above expansion via the equation

$$M^{(0...1...0)}(z) = \frac{\partial}{\partial x_i} M(z,0) , \tag{3.46}$$

where the index $i$ is the position of the 1 in the expression $M^{(0...1...0)}(z)$. The entry $M_{v_i w}^{(0...1...0)}(z)$ then corresponds to the transfer function for what enters the sink $v_i$ from vertex $w$ before disappearing. For the example given in figure 3, this corresponds to

$$M^{(1)}(z) = \begin{bmatrix} z^{-2} & z^{-1} \\ z^{-3} & z^{-2} \end{bmatrix} , \tag{3.47}$$

which matches our expectations, since if a signal is introduced at vertex 1, there is a time delay of 2 before it returns and vanishes. If a signal is introduced at vertex 2, there is a time delay of 1 before it propagates to vertex 1 and vanishes.

3.3. **The Walk Representation of the Transfer Matrix.** Before we return to our derivation of the full transfer matrix $M(z)$ for a 1-D symmetric grid in section 3.1, we will shortly address the walk representation of the transfer matrix $M(z)$. This representation is very simple, it states that the transfer function $M_{uv}(z)$ is the sum over all transfer functions of all walks on the graph $G$ from vertex $v$ to vertex $u$. The derivation is immediate from eq. (2.8),

$$M_{uv}(z) = \delta_{uv} + T_{uv}(z) + \sum_{w_1} T_{uw_1}(z)T_{w_1v}(z) + \sum_{w_1w_2} T_{uw_2}(z)T_{w_2w_1}(z)T_{w_1v}(z) + \dots , \tag{3.48}$$

Alternatively, we write this using different notation

$$M_{uv}(z) = \sum_{w:v\to u} \prod_{i=0}^{l-1} T_{w_iw_{i+1}}(z) = \sum_{w:v\to u} T_w(z) , \tag{3.49}$$

where the sum is over all walks $w = w_0w_1w_2...w_l$ from $v$ to $u$ in $G$, and $M_\omega(z)$ is the transfer function of the walk $w$, defined as the product of the transfer functions of the individual edges of $w$. Similarly, the modified transfer matrix $M(z,x)$ with marked vertices $v_1, v_2, ..., v_m$ can be easily derived from eq. (3.31),

$$M_{uv}(z,x) = \sum_{\omega:v\to u} \prod_{i=0}^{l-1} T_{w_iw_{i+1}}(z) \prod_{j=1}^{m} (x_j)^{\delta_{v_jw_{i+1}}} = \sum_{\omega:v\to u} x_1^{c_1}x_2^{c_2}...x_m^{c_m}T_w(z) , \tag{3.50}$$

where $c_i$ is the number of times the walk $w$ enters the marked vertex $v_i$. In the above representation, we can decompose $M_{uv}(z)$ by whether the walk $w$ ever enters the vertex $v_i$ or not. Let $W_0$ be the set of walks that never enter $v_i$ and let $W_i$ be the set of walks that terminate at $v_i$ but never enter $v_i$ before termination. Then, we have

$$M_{uv}(z,x) = \sum_{w\in W_0} x_2^{c_2}...x_m^{c_m}T_w(z) + \sum_{w\in W_i} x_1^{a_1}x_2^{a_2}...x_m^{a_m}T_w(z) \sum_{w':v_i\to u} x_1^{b_1}x_2^{b_2}...x_m^{b_m}T_{w'}(z) , \tag{3.51}$$

where $a_i = 1$ and we have split the walks in the set $W_i$ into two components. Every walk in $W_i$ can be decomposed into two walks $w$ and $w'$, where $w$ is a walk terminating at $v_1$ which never enters $v_i$ before it terminates and $w'$ is an arbitrary walk from $v_i$ to $u$. Essentially, we chop off the first part of the walk before $v_i$. $a_1, a_2, ..., a_m$ and $b_1, b_2, ..., b_m$ are the corresponding marked vertex counts in $w$ and $w'$ respectively. We can now rewrite the above equation as

$$M_{uv}(z,x) = [M_{uv}(z,x)]_{x_i=0} + x_i \left[\frac{\partial}{\partial x_i} M_{v_iv}(z,x)\right]_{x_i=0} M_{uv_i}(z,x) . \tag{3.52}$$

Since $u$ and $v$ were chosen arbitrary, this can be written in operator form,

$$M(z,x) = [M(z,x)]_{x_i=0} + x_iM(z,x)P_{v_i} \left[\frac{\partial}{\partial x_i} M(z,x)\right]_{x_i=0} . \tag{3.53}$$

Note that a similar expression can be derived by expanding the identity (3.38). However, this method of derivation makes the underlying intuition clearer. Iterating the above equation for $x_1, x_2, x_3, ..., x_N$ gives

$$\begin{aligned} M(z,x) = \sum_{i=1}^{N} x_1...x_{i-1} \left[M(z,x)\right]_{x_i=0} P_{v_{i-1}} \left[\frac{\partial}{\partial x_{i-1}} M(z,x)\right]_{x_{i-1}=0} P_{v_{i-2}}...P_{v_1} \left[\frac{\partial}{\partial x_1} M(z,x)\right]_{x_1=0} \\ + x_1x_2...x_NM(z,x)P_{v_N} \left[\frac{\partial}{\partial x_N} M(z,x)\right]_{x_N=0} P_{v_{N-1}}...P_{v_1} \left[\frac{\partial}{\partial x_1} M(z,x)\right]_{x_1=0} . \end{aligned} \tag{3.54}$$

A similar decomposition can be performed simultaneously for all marked vertices $v_1, v_2, ..., v_m$ by splitting the walks based on which marked vertex they enter first, i.e.,

$$M_{uv}(z,x) = \sum_{w\in W_0} T_w(z) + \sum_{i=1}^{m}\sum_{w\in W_i} x_1^{a_{i,1}}x_2^{a_{i,2}}...\,x_i\,...x_m^{a_{i,m}}T_w(z)\sum_{w':v_i\to u} x_1^{b_1}x_2^{b_2}...x_m^{b_m}T_{w'}(z)\,, \tag{3.55}$$

where $W_i$ is the set of walks that terminate at $v_i$ and never enter either $v_i$ or any of the other marked vertices before termination, and $W_0$ is the set of walks which never enter any $v_i$. In analogy to eq. (3.52), this becomes

$$M_{uv}(z,x) = M_{uv}(z,0) + \sum_{i=1}^{m} x_i\left[\frac{\partial}{\partial x_i}M_{v_iu}(z,0)\right]M_{uv_i}(z,x)\,. \tag{3.56}$$

In operator form, the above can be written

$$M(z,x) = M(z,0) + \sum_{i=1}^{m} x_i M(z,x)P_{v_i}\frac{\partial}{\partial x_i}M(z,0)\,. \tag{3.57}$$

Note that eq. (3.57) can also be derived from eq. (3.38).

Eq. (3.57) gives us a practical method of computing what enters the sink vertices $v_1, ..., v_n$. Setting $x_i = 1$ in eq. (3.57) results in

$$M(z) = M(z,0) + \sum_{i=1}^{m} M(z)P_{v_i}\frac{\partial}{\partial x_j}M(z,0)\,. \tag{3.58}$$

Taking the $v_iv$ matrix entry of the above equation for arbitrary non-marked vertex $v$ provides

$$M_{v_iv}(z) = M_{v_iv}(z,0) + \sum_{j=1}^{m} M_{v_iv_j}(z)\frac{\partial}{\partial x_j}M_{v_jv}(z,0)\,. \tag{3.59}$$

Since $v$ is not marked, we know that $M_{v_iv}(z,0) = \delta_{v_iv} = 0$. Defining the desired quantity

$$H_{v_jv}(z) \equiv \frac{\partial}{\partial x_j}M_{v_jv}(z,0)\,, \tag{3.60}$$

eq. (3.59) becomes a matrix equation,

$$\begin{bmatrix} M_{v_1v}(z) \\ M_{v_2v}(z) \\ \vdots \\ M_{v_mv}(z) \end{bmatrix} = \begin{bmatrix} M_{v_1v_1}(z) & M_{v_1v_2}(z) & ... & M_{v_1v_m}(z) \\ M_{v_2v_1}(z) & M_{v_2v_2}(z) & ... & M_{v_2v_m}(z) \\ \vdots & \vdots & \ddots & \vdots \\ M_{v_mv_1}(z) & M_{v_mv_2}(z) & ... & M_{v_mv_m}(z) \end{bmatrix}\begin{bmatrix} H_{v_1v}(z) \\ H_{v_2v}(z) \\ \vdots \\ H_{v_mv}(z) \end{bmatrix}, \tag{3.61}$$

which means that we can solve for the individual $H_{v_jv}(z)$ by inverting the above linear system,

$$\begin{bmatrix} H_{v_1v}(z) \\ H_{v_2v}(z) \\ \vdots \\ H_{v_mv}(z) \end{bmatrix} = \begin{bmatrix} M_{v_1v_1}(z) & M_{v_1v_2}(z) & ... & M_{v_1v_m}(z) \\ M_{v_2v_1}(z) & M_{v_2v_2}(z) & ... & M_{v_2v_m}(z) \\ \vdots & \vdots & \ddots & \vdots \\ M_{v_mv_1}(z) & M_{v_mv_2}(z) & ... & M_{v_mv_m}(z) \end{bmatrix}^{-1}\begin{bmatrix} M_{v_1v}(z) \\ M_{v_2v}(z) \\ \vdots \\ M_{v_mv}(z) \end{bmatrix}. \tag{3.62}$$

3.4. **Return to Symmetric Grid Graphs in Dimension One.** We now return to finish what we started in section 3.1. We mark all vertices $v_i$ with a corresponding dummy variable $x_i$ as discussed in the section 3.2 and 3.3. To compute the full matrix $M_{uv}(z)$, it suffices to compute $M_{N0}(z)$ for $N \geq 1$. This is where we will use the decomposition (3.54). Note that the summation term in the decomposition corresponds to all walks which do not enter at least one of the vertices 1, 2, ..., $N$.

However, since in dimension one we must necessarily enter all of these vertices to reach the vertex $N$, the summation term vanishes in the $0N$-entry of $M(z,x)$, leaving us with

$$M_{N0}(z,x) = x_1 x_2 ... x_N M_{NN}(z,x) \prod_{i=1}^{N} \left[ \frac{\partial}{\partial x_i} M_{i,i-1}(z,x) \right]_{x_i=0} . \tag{3.63}$$

Computing $M_{N0}(z)$ requires letting $x_i = 1$ for all $x_i$. This transforms the above into

$$M_{N0}(z) = S(z) \prod_{i=1}^{N} \frac{\partial}{\partial x_i} M_{i,i-1}(z, ..., 1, 0, 1, ...) . \tag{3.64}$$

where the 0 occurs at the $x_i$ input of $M_{i,i-1}$. However, note that the translation invariance of the system demands that all $\frac{\partial}{\partial x_i} M_{i,i-1}(z, ..., 1, 0, 1, ...)$ are identical. As such, the above equation can be rewritten once again as

$$M_{N0}(z) = S(z) L(z)^N . \tag{3.65}$$

It only remains to derive the quantity $L(z)$. This is fairly easy, since we've already calculated $N(z) = M_{01}(z)$ in eq. (3.25),

$$S(z)L(z) = N(z) = \frac{S(z) - 1}{2\Omega(z)} , \tag{3.66}$$

resulting in

$$L(z) = \frac{S(z) - 1}{2\Omega(z) S(z)} . \tag{3.67}$$

Using eq. (3.65), we arrive at a closed form solution for the transfer matrix $M(z)$,

$$M_{ij}(z) = S(z) \left[ \frac{S(z) - 1}{2\Omega(z) S(z)} \right]^{|i-j|} , \tag{3.68}$$

where $S(z)$ can be calculated using the approach in eq. (3.18). The propagator is

$$K(z; \xi) = 2\Omega(z) \cos(2\pi\xi) . \tag{3.69}$$

Therefore, as per eq. (3.18), $S(z)$ is given by

$$S(z) = 2\pi i \sum_{\xi_k} \mathrm{res}_{\xi \to \xi_k} \frac{1}{1 - 2\Omega(z) \cos(2\pi\xi)} . \tag{3.70}$$

As an example, for a simple random walk on $\mathbb{Z}$, this procedure provides

$$M_{ij}(z) = \frac{z^{|i-j|}}{\sqrt{1 - z^{-2}}} \left[ 1 - \sqrt{1 - z^{-2}} \right]^{|i-j|} \tag{3.71}$$

3.4.1. *Symmetric Grid Graphs in Dimension One with Self-Loops.* There are also situations which may arise where the underlying graph may have self loops in addition to the structure we've already examined. That is, where our generators are given by $g_0 = 0$, $g_1 = 1$, $g_2 = -1$. The extra $g_0$ generator gives self loops on all the edges. For symmetry, we once again require that

$$\Omega(z) \equiv \Omega_1(z) = \Omega_{-1}(z) . \tag{3.72}$$

However, the transfer function $\Omega_0(z)$ corresponding to $g_0$ may be arbitrary. The resulting propagation system can be easily analyzed with the same approach. The propagator becomes

$$K(\xi; z) = 2\Omega(z) \cos(2\pi\xi) + \Omega_0(z) . \tag{3.73}$$

The self-transfer function $S(z)$ can be computed again with residue calculus,

$$S(z) = \int_{-1/2}^{1/2} \frac{1}{1 - 2\Omega(z)\cos(2\pi\xi) - \Omega_0(z)} \, d\xi = 2\pi i \sum_{\xi_k} \mathrm{res}_{\xi \to \xi_k} \frac{1}{1 - 2\Omega(z)\cos(2\pi\xi) - \Omega_0(z)} . \tag{3.74}$$

If $N(z)$ is the neighbor transfer function, we have

$$S(z) = 2\Omega(z)N(z) + \Omega_0(z)S(z) + 1\,, \tag{3.75}$$

which gives

$$N(z) = \frac{S(z)\Omega_0(z) + S(z) + 1}{2\Omega(z)}\,. \tag{3.76}$$

To reach a vertex $u$ from another vertex $v$, we must pass through all of the vertices in between. Therefore, the analysis of the previous section still holds, and the transfer matrix can be computed exactly. Using eqs. (3.65) and (3.66), the result is

$$M_{ij}(z) = S(z)\left[\frac{S(z)\Omega_0(z) + S(z) + 1}{2\Omega(z)S(z)}\right]^{|i-j|}\,. \tag{3.77}$$

3.5. **Reduction to Dimension One.** It is possible to recover information about propagation on graphs in higher dimensions by using the technique described in the previous section, if the graph meets certain properties. This can be done by splitting the graph $G$ in $d$ dimensions into an infinite number of lateral $d-1$-dimensional slices. By treating each of these slices as its own vertex and collapsing the graph $G$ onto these vertices, the result is a graph in dimension one – enabling us to use the results of the previous section if the resulting graph has specific properties. Suppose that the $d$th dimension is the direction orthogonal to the slices, that is each slice corresponds to the vertex set $\mathbb{Z}^{d-1} \times v_d$. Then, the requirements for the collapse procedure forming a symmetric grid graph in dimension one are as follows:

(1) *Locality*: for every $\boldsymbol{g} = (v_1, v_2, ..., v_d)$, we must have $|v_d| \leq 1$.
(2) *Symmetry*: for every $\boldsymbol{g} = (v_1, v_2, ..., v_d)$ in the set of generators $\mathcal{G}$, there must be a corresponding generator $\boldsymbol{g}' = (v_1, v_2, ..., -v_d)$ in $\mathcal{G}$. Moreover, $\boldsymbol{g}$ and $\boldsymbol{g}'$ must have the same transfer function, $\Omega_{\boldsymbol{g}}(z) = \Omega_{\boldsymbol{g}'}(z)$.

Condition (1) ensures that the resulting collapsed graph formed is indeed a grid graph on $\mathbb{Z}$ (or in the degenerate case, the trivial Cayley graph on $\mathbb{Z}$), and condition (2) ensures that we have symmetry on the resulting collapsed graph, that is, $\Omega_1(z) = \Omega_{-1}(z)$.

The collapse procedure is done as follows. Consider the propagation of a $d-1$-dimensional plane wave on $G$, that is, with input signal

$$\Phi_{(v_1,v_2,...,v_{d-1},v_d)}(z) = e^{2\pi i \Xi_1 v_1} e^{2\pi i \Xi_2 v_2} ... e^{2\pi i \Xi_{d-1} v_{d-1}} \delta[v_d]\,, \tag{3.78}$$

where $\delta$ is the discrete Dirac delta function, and $\Xi_1, \Xi_2, ..., \Xi_{d-1}$ are the corresponding frequencies of the plane wave. This initial data corresponds to a plane wave on the plane $\mathbb{Z}^{d-1} \times 0$ at time $t = 0$. If the conditions (1) and (2) are met, then the propagator can be written as

$$K(\boldsymbol{\xi}; z) = K_1(\xi_1, ..., \xi_{d-1}; z)\cos(2\pi\xi_d) + K_0(\xi_1, ..., \xi_{d-1}; z)\,. \tag{3.79}$$

Therefore, we can compute the results of propagation by applying the propagator to the Fourier transform of the input signal,

$$\hat{\Phi}(\boldsymbol{\xi}; z) = \delta[\xi_1 - \Xi_1]\,\delta[\xi_2 - \Xi_2]\,...\,\delta[\xi_{d-1} - \Xi_{d-1}]\,. \tag{3.80}$$

It follows from eq. (3.4) that the system state $\Psi$ is given by

$$\begin{aligned}\Psi_{(v_1,v_2,...,v_{d-1},v_d)}(z) &= \int_{-1/2}^{1/2} \frac{e^{2\pi i \boldsymbol{\xi}\cdot\boldsymbol{v}}}{1 - K(\boldsymbol{\xi}; z)} \hat{\Phi}(\boldsymbol{\xi}; z)\, d^n\xi \\ &= \prod_{j=1}^{d-1} e^{2\pi i \Xi_j v_j} \int_{-1/2}^{1/2} \frac{e^{2\pi i \xi_d v_d}}{1 - K(\Xi_1, ..., \Xi_{d-1}, \xi_d; z)}\, d\xi_d\,.\end{aligned} \tag{3.81}$$

Thus, we let $\zeta_v(\Xi_1, ..., \Xi_{d-1}; z)$ be defined by the Fourier coefficient z-transform given by

$$\zeta_v(\Xi_1, ..., \Xi_{d-1}; z) \equiv \int_{-1/2}^{1/2} \frac{e^{2\pi i \xi_d v}}{1 - K(\Xi_1, ..., \Xi_{d-1}, \xi_d; z)} \, d\xi_d \,. \tag{3.82}$$

This gives

$$\Psi_{(v_1, v_2, ..., v_{d-1}, v_d)}(z) = \zeta_{v_d}(\Xi_1, ..., \Xi_{d-1}; z) \prod_{j=1}^{d-1} e^{2\pi i \Xi_j v_j} \tag{3.83}$$

then we can see that the propagation of $\zeta_v(\Xi_1, ..., \Xi_{d-1}; z)$ is equivalent to propagation on a symmetric grid graph of dimension one (as seen in section 3.4.1) with generators $g_0 = 0, g_1 = 1, g_2 = -1$ and

$$\Omega_0(z) = K_0(\Xi_1, ..., \Xi_{d-1}; z) \,, \qquad \Omega(z) = K_1(\Xi_1, ..., \Xi_{d-1}; z) \,. \tag{3.84}$$

Thus, using eq. (3.77), the phase factor z-transform can be computed to be

$$\zeta_v(\Xi_1, ..., \Xi_{d-1}; z) = S(z) \left[ \frac{S(z) K_0(\Xi_1, ..., \Xi_{d-1}; z) + S(z) + 1}{2 K_1(\Xi_1, ..., \Xi_{d-1}; z) S(z)} \right]^{|v|} \,, \tag{3.85}$$

where

$$S(z) = 2\pi i \sum_{\xi_k} \mathrm{res}_{\xi \to \xi_k} \frac{1}{1 - 2K_1(\Xi_1, ..., \Xi_{d-1}; z) \cos(2\pi\xi) - K_0(\Xi_1, ..., \Xi_{d-1}; z)} \,. \tag{3.86}$$

Since propagation on the graph is linear, the phase factor in eq. (3.85) is precisely the sum of transfer functions between two slices of the graph in the Fourier domain at different times. That is,

$$\zeta_v(\xi_1, ..., \xi_{d-1}; z) = \sum_{t=0}^{\infty} \hat{F}_v^{(t)}(\xi_1, ..., \xi_{d-1}) z^{-t} \,, \tag{3.87}$$

where $\hat{F}_v^{(t)}$ is the transfer function at time delay $t$ between two layers a distance $v$ apart. We can extract useful information from this function. For example, we can obtain the sum of the individual transfer functions by taking

$$\sum_{t=0}^{\infty} \hat{F}_v^{(t)}(\xi_1, ..., \xi_{d-1}) = \zeta_v(\xi_1, ..., \xi_{d-1}; 1) \,. \tag{3.88}$$

If the propagation on the system involves interference, i.e. the transfer functions ascribed to the edges of the graph have complex valued coefficients, we can also ask for the total power of the transfer function at some frequency using Parseval's identity,

$$\sum_{t=0}^{\infty} |\hat{F}_v^{(t)}(\xi_1, ..., \xi_{d-1})|^2 = \int_0^1 |\zeta_v(\xi_1, ..., \xi_{d-1}; e^{2\pi i x})|^2 \, dx \,. \tag{3.89}$$

If the time step is presumed to be infinitesimal then the above quantity corresponds approximately to how much the incoming signal is damped by propagating from one slice to another slice a distance $v$ away.

3.6. **Propagation in a Thin Layer.** The problem with the model we have used until this point is that the area in which the signal scatters is effectively infinite. But the situation we would like to model is the propagation of light through a thin layer. We would like to imagine that a signal enters the layer through one end and we would like to recover the signal which exists at the other – or rather, the corresponding transfer function between these two signals. The desired scenario is shown in figure 4.

The models we have looked at are not fully able to capture the behavior in figure 4 because any part of the signal that leaves a region of the graph can propagate back into the region later. We would like to find a way to stop this back propagation entirely. This can be done using the machinery

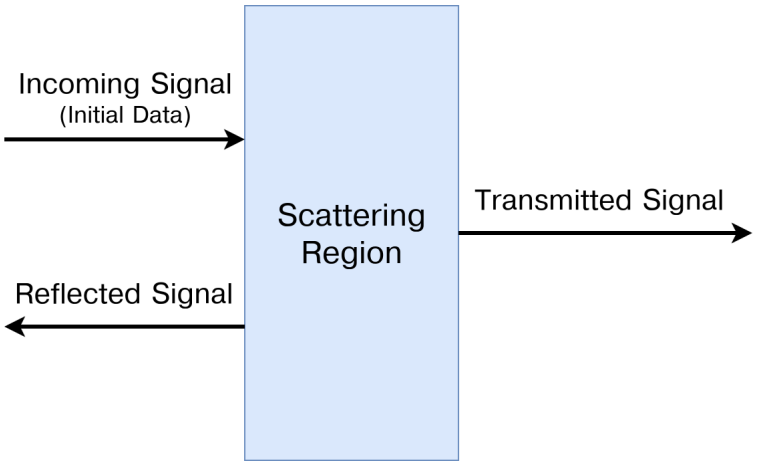


FIGURE 4. The scenario we are trying to model. There is a thin layer which scatters an incoming signal from the left side of the region. We would like to determine transfer functions for the signal transmitted through the region and the signal reflected back.

FIGURE 5. Scattering model in dimension one. The gray vertices denote sinks and the orange vertex is the source vertex for a signal entering the scattering region from the left. As per figure 4, we would like recover what exits the system at the right end of the region, at the rightmost gray vertex.

of sinks introduced in section 3.2. Specifying a layer of the graph as the scattering region, we place sinks at either ends of the region, as seen in figure 5. Whatever parts of the signal arrive at these sinks are then removed from the system and will no longer propagate back into the scattering region. Our goal is then to recover what leaves the system at either end of the scattering region (see the discussion at the end of section 3.2). We introduce a signal at some chosen source vertex in the graph, typically neighboring one of the sinks (see the orange vertex in figure 5). If we call this source $s$ and the two sinks $v_1$ and $v_2$, with dummy variables $x_1$ and $x_2$ respectively, then we want to recover $H_R(z) \equiv H_{v_1 s}(z)$ and $H_T(z) \equiv H_{v_2 s}(z)$ from eq. (3.60), as these are the transfer functions corresponding to the reflected and transmitted signals respectively.

Eq. (3.62) tells us that

$$\begin{bmatrix} H_R(z) \\ H_T(z) \end{bmatrix} = \begin{bmatrix} M_{v_1 v_1}(z) & M_{v_1 v_2}(z) \\ M_{v_2 v_1}(z) & M_{v_2 v_2}(z) \end{bmatrix}^{-1} \begin{bmatrix} M_{v_1 s}(z) \\ M_{v_2 s}(z) \end{bmatrix}. \tag{3.90}$$

Hence, if we let $v_1 = 0$, $v_2 = D$, where $D$ is the length of the layer, then we have

$$\begin{bmatrix} H_R(z) \\ H_T(z) \end{bmatrix} = \begin{bmatrix} 1 & L(z)^D \\ L(z)^D & 1 \end{bmatrix}^{-1} \begin{bmatrix} L(z)^s \\ L(z)^{D-s} \end{bmatrix}, \tag{3.91}$$

where

$$L(z) = \frac{S(z)\Omega_0(z) + S(z) + 1}{2\Omega(z)S(z)}, \tag{3.92}$$

and from (3.74), we obtain

$$S(z) = 2\pi i \sum_{\xi_k} \operatorname{res}_{\xi \to \xi_k} \frac{1}{1 - 2\Omega(z)\cos(2\pi\xi) - \Omega_0(z)}. \tag{3.93}$$

For models with dimension $d > 1$, we can use the procedure in section 3.5 to reduce to the one dimensional case and then use eq. (3.91) to recover the transfer function $\hat{F}(\Xi_1, ..., \Xi_{d-1}; z) = H_T(\xi_1, ..., \xi_{d-1}; z)$ from one end of the scattering region to the other. That is,

(3.94)
$$\begin{bmatrix} H_R(\xi_1, ..., \xi_{d-1}; z) \\ H_T(\xi_1, ..., \xi_{d-1}; z) \end{bmatrix} = \begin{bmatrix} 1 & L(\xi_1, ..., \xi_{d-1}; z)^D \\ L(\xi_1, ..., \xi_{d-1}; z)^D & 1 \end{bmatrix}^{-1} \begin{bmatrix} L(\xi_1, ..., \xi_{d-1}; z)^s \\ L(\xi_1, ..., \xi_{d-1}; z)^{D-s} \end{bmatrix},$$

where

$$L(\xi_1, ..., \xi_{d-1}; z) = \frac{S(z)K_0(\xi_1, ..., \xi_{d-1}; z) + S(z) + 1}{2K_1(\xi_1, ..., \xi_{d-1}; z)S(z)}, \tag{3.95}$$

and from eq. (3.86),

$$S(z) = 2\pi i \sum_{\xi_k} \text{res}_{\xi \to \xi_k} \frac{1}{1 - 2K_1(\xi_1, ..., \xi_{d-1}; z)\cos(2\pi\xi) - K_0(\xi_1, ..., \xi_{d-1}; z)}. \tag{3.96}$$

## 4. Scattering models with direction

One of the problems with the above models is that a signal coming into a vertex is scattered in the same way irrespective of the incidence direction. However, some physical processes like Mie scattering have an explicit dependence on direction, i.e. a scattered particle is more likely to continue in the same direction than it is to reverse direction. Accounting for these types of processes requires a non-trivial modification to the above model. We still begin with a Cayley graph $G$ on $\mathbb{Z}^d$ with generators $\mathcal{G} = \{\boldsymbol{g}_1, ..., \boldsymbol{g}_k\}$, but now we associate a transfer function $\Omega_{\boldsymbol{gh}}(z)$ to each pair of generators $\boldsymbol{g}, \boldsymbol{h} \in \mathcal{G}$ with the understanding that the function $\Omega_{\boldsymbol{gh}}(z)$ is applied to a signal when it propagates through an edge corresponding to $\boldsymbol{g}$ if it previously propagated through an edge corresponding to $\boldsymbol{h}$. In the state of our system, we now have to explicitly account for the direction from which a signal enters a node. Hence, the system state is given by a tensor of functions $\Psi^{\boldsymbol{g}}_{\boldsymbol{v}}(z)$ where $\boldsymbol{v} \in \mathbb{Z}^d$ is the vertex at which the signal $\Psi^{\boldsymbol{g}}_{\boldsymbol{v}}(z)$ is seen and $\boldsymbol{g} \in \mathcal{G}$ is the corresponding entrance direction. The cumulative signal seen by a vertex is then given by summing over all entrance directions,

$$\Psi_{\boldsymbol{v}}(z) = \sum_{\boldsymbol{g} \in \mathcal{G}} \Psi^{\boldsymbol{g}}_{\boldsymbol{v}}(z). \tag{4.1}$$

The governing equations of the system are given by

$$\Psi^{\boldsymbol{g}}_{\boldsymbol{v}}(z) = \sum_{\boldsymbol{h} \in \mathcal{G}} \Omega_{\boldsymbol{gh}}(z)\Psi^{\boldsymbol{h}}_{\boldsymbol{v}-\boldsymbol{h}}(z) + \Phi^{\boldsymbol{g}}_{\boldsymbol{v}}(z), \tag{4.2}$$

where $\Phi^{\boldsymbol{g}}_{\boldsymbol{v}}(z)$ is the input signal at vertex $\boldsymbol{v}$ and in direction $\boldsymbol{g}$. Note that this is essentially a propagation graph on $\mathbb{Z}^d \times \mathcal{G}$. Again, for each generator $\boldsymbol{g} \in \mathcal{G}$, we define the spatial Fourier transform $\hat{\Psi}^{\boldsymbol{g}}$ as

$$\hat{\Psi}^{\boldsymbol{g}}(\boldsymbol{\xi}; z) = \sum_{\boldsymbol{v} \in \mathbb{Z}^d} e^{-2\pi i \boldsymbol{\xi} \cdot \boldsymbol{v}} \Psi^{\boldsymbol{g}}_{\boldsymbol{v}}(z). \tag{4.3}$$

The spatial Fourier transform of the governing equations now gives

$$\hat{\Psi}^{\boldsymbol{g}}(\boldsymbol{\xi}; z) = \sum_{\boldsymbol{h} \in \mathcal{G}} \Omega_{\boldsymbol{gh}}(z) e^{2\pi i \boldsymbol{h} \cdot \boldsymbol{\xi}} \hat{\Psi}^{\boldsymbol{h}}(\boldsymbol{\xi}; z) + \hat{\Phi}^{\boldsymbol{g}}(\boldsymbol{\xi}; z). \tag{4.4}$$

Defining

$$\hat{\Psi}(\boldsymbol{\xi}; z) \equiv \begin{bmatrix} \hat{\Psi}^{\boldsymbol{g}_1}(\boldsymbol{\xi}; z) \\ \hat{\Psi}^{\boldsymbol{g}_2}(\boldsymbol{\xi}; z) \\ \vdots \\ \hat{\Psi}^{\boldsymbol{g}_k}(\boldsymbol{\xi}; z) \end{bmatrix}, \qquad \hat{\Phi}(\boldsymbol{\xi}; z) \equiv \begin{bmatrix} \hat{\Phi}^{\boldsymbol{g}_1}(\boldsymbol{\xi}; z) \\ \hat{\Phi}^{\boldsymbol{g}_2}(\boldsymbol{\xi}; z) \\ \vdots \\ \hat{\Phi}^{\boldsymbol{g}_k}(\boldsymbol{\xi}; z) \end{bmatrix}. \tag{4.5}$$

Eq. (4.4) can then be written as a matrix equation,

$$\hat{\Psi}(\boldsymbol{\xi};z) = \begin{bmatrix} \Omega_{\boldsymbol{g}_1\boldsymbol{g}_1}(z)e^{2\pi i\boldsymbol{g}_1\cdot\boldsymbol{\xi}} & \Omega_{\boldsymbol{g}_1\boldsymbol{g}_2}(z)e^{2\pi i\boldsymbol{g}_2\cdot\boldsymbol{\xi}} & \dots & \Omega_{\boldsymbol{g}_1\boldsymbol{g}_k}(z)e^{2\pi i\boldsymbol{g}_k\cdot\boldsymbol{\xi}} \\ \Omega_{\boldsymbol{g}_2\boldsymbol{g}_1}(z)e^{2\pi i\boldsymbol{g}_1\cdot\boldsymbol{\xi}} & \Omega_{\boldsymbol{g}_2\boldsymbol{g}_2}(z)e^{2\pi i\boldsymbol{g}_2\cdot\boldsymbol{\xi}} & \dots & \Omega_{\boldsymbol{g}_2\boldsymbol{g}_k}(z)e^{2\pi i\boldsymbol{g}_k\cdot\boldsymbol{\xi}} \\ \vdots & \vdots & \ddots & \vdots \\ \Omega_{\boldsymbol{g}_k\boldsymbol{g}_1}(z)e^{2\pi i\boldsymbol{g}_1\cdot\boldsymbol{\xi}} & \Omega_{\boldsymbol{g}_k\boldsymbol{g}_2}(z)e^{2\pi i\boldsymbol{g}_2\cdot\boldsymbol{\xi}} & \dots & \Omega_{\boldsymbol{g}_k\boldsymbol{g}_k}(z)e^{2\pi i\boldsymbol{g}_k\cdot\boldsymbol{\xi}} \end{bmatrix} \hat{\Psi}(\boldsymbol{\xi};z) + \hat{\Phi}(\boldsymbol{\xi};z)\,. \tag{4.6}$$

We define the propagator matrix $K(\boldsymbol{\xi};z)$ as the matrix in the above expression. The solution for $\hat{\Psi}(\boldsymbol{\xi};z)$ is then

$$\hat{\Psi}(\boldsymbol{\xi};z) = (I - K(\boldsymbol{\xi};z))^{-1}\hat{\Phi}(\boldsymbol{\xi};z)\,. \tag{4.7}$$

Taking the inverse Fourier transform,

$$\Psi_{\boldsymbol{v}}(z) = \int_{-1/2}^{1/2} e^{2\pi i\boldsymbol{\xi}\cdot\boldsymbol{v}}(I - K(\boldsymbol{\xi};z))^{-1}\hat{\Phi}(\boldsymbol{\xi};z)\,d\boldsymbol{\xi} = \sum_{\boldsymbol{w}\in\mathbb{Z}^d}\int_{-1/2}^{1/2} e^{2\pi i\boldsymbol{\xi}\cdot(\boldsymbol{v}-\boldsymbol{w})}(I - K(\boldsymbol{\xi};z))^{-1}\,d\boldsymbol{\xi}\,\Phi_{\boldsymbol{\omega}}(z)\,, \tag{4.8}$$

where $\Psi_{\boldsymbol{v}}(z)$ is the vector indexed in $\mathcal{G}$, with entries $\Psi^{\boldsymbol{g}}_{\boldsymbol{v}}(z)$. From the above equation, the transfer tensor $M(z)$ then takes the form

$$M^{\boldsymbol{g}\boldsymbol{h}}_{\boldsymbol{v}\boldsymbol{w}}(z) = \left[\int_{-1/2}^{1/2} e^{2\pi i\boldsymbol{\xi}\cdot(\boldsymbol{v}-\boldsymbol{w})}(I - K(\boldsymbol{\xi};z))^{-1}\,d\boldsymbol{\xi}\right]_{\boldsymbol{g}\boldsymbol{h}}\,. \tag{4.9}$$

Note that the tensor $M(z)$ is indexed by $\boldsymbol{v},\boldsymbol{w}\in\mathbb{Z}^d$ and $\boldsymbol{g},\boldsymbol{h}\in\mathcal{G}$, and its entries represent the transfer functions for a signal propagating from vertex $\boldsymbol{w}$ with direction $\boldsymbol{g}$ to vertex $\boldsymbol{v}$ with direction $\boldsymbol{h}$, i.e.,

$$\Psi^{\boldsymbol{g}}_{\boldsymbol{v}}(z) = \sum_{\boldsymbol{w}\in\mathbb{Z}^d}\sum_{\boldsymbol{h}\in\mathcal{G}} M^{\boldsymbol{g}\boldsymbol{h}}_{\boldsymbol{v}\boldsymbol{w}}(z)\Phi^{\boldsymbol{h}}_{\boldsymbol{w}}(z)\,. \tag{4.10}$$

If the system is viewed as a propagation graph on the vertex set $\mathbb{Z}^d\times\mathcal{G}$, then $M^{\boldsymbol{g}\boldsymbol{h}}_{\boldsymbol{v}\boldsymbol{w}}(z)$ can be interpreted as a matrix.

4.1. **Symmetric Grids in Dimension One.** In analogy to section 3.1, we would like to compute the entries of the transfer matrix $M(z)$ when $d=1$ and when the system is symmetric. Once again, we have generators $g_0=0, g_1=1, g_2=-1$. Furthermore, for the resulting system to be symmetric, we must have

$$\Omega_{g,h}(z) = \Omega_{-g,-h}(z)\,. \tag{4.11}$$

If we view the resulting system as a propagation graph on the vertex set $\mathbb{Z}\times\{-1,0,1\}$, we obtain the propagation graph shown in figure 6.

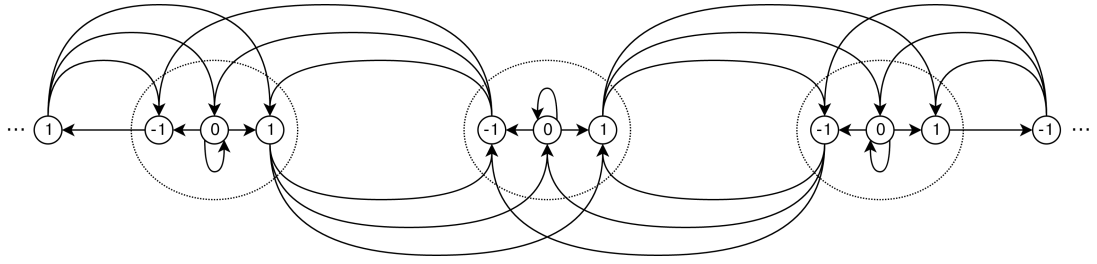


FIGURE 6. Symmetric grid graph in dimension one with directional scattering. Note that each vertex on $\mathbb{Z}$ (denoted by dotted circles) is expanded into three individual vertices corresponding to scattering direction.

To derive transfer functions, we perform an analysis similar to section 3. We would like to compute the matrix entries $M_{0N}^{1,1}(z)$ as well as $M_{0N}^{-1,1}(z)$, since these will suffice to compute transfer functions for propagation in a thin layer. Our method of computation relies on clever use of the symmetry of the graph. First, consider input to the system given by

$$\Phi_v^g(z) = \frac{1}{2}\left(\delta[v]\delta_{g,1} + \delta[v]\delta_{g,-1}\right) , \tag{4.12}$$

that is, we start with two half unit pulses at vertices $(0,1)$ and $(0,-1)$. Due to this initial data, the system in figure 6 is always symmetric with respect to a flip about the vertex $(0,0)$, which means

$$\Psi_v^g(z) = \Psi_{-v}^{-g}(z) . \tag{4.13}$$

Thus, we define

$$\begin{aligned}
S_0^{\mathrm{sym}}(z) &\equiv \Psi_0^0(z) \\
S_1^{\mathrm{sym}}(z) &\equiv \Psi_0^1(z) = \Psi_0^{-1}(z) , \\
N_{-1}^{\mathrm{sym}}(z) &\equiv \Psi_1^{-1}(z) = \Psi_{-1}^1(z) , \\
N_0^{\mathrm{sym}}(z) &\equiv \Psi_1^0(z) = \Psi_{-1}^0(z) , \\
N_1^{\mathrm{sym}}(z) &\equiv \Psi_1^1(z) = \Psi_{-1}^{-1}(z) , \\
U_{-1}^{\mathrm{sym}}(z) &\equiv \Psi_2^{-1}(z) = \Psi_{-2}^1(z) .
\end{aligned} \tag{4.14}$$

Looking at figure 6, we can write down expressions for the above using eqs. (4.2), these become

$$\begin{aligned}
S_0^{\mathrm{sym}}(z) &= \Omega_{0,1}(z)N_{-1}^{\mathrm{sym}}(z) + \Omega_{0,-1}(z)N_{-1}^{\mathrm{sym}}(z) + \Omega_{0,0}(z)S_0^{\mathrm{sym}}(z) + \frac{1}{2} , \\
S_1^{\mathrm{sym}}(z) &= \Omega_{1,1}(z)N_{-1}^{\mathrm{sym}}(z) + \Omega_{1,-1}(z)N_{-1}^{\mathrm{sym}}(z) + \Omega_{1,0}(z)S_0^{\mathrm{sym}}(z) , \\
N_{-1}^{\mathrm{sym}}(z) &= \Omega_{-1,1}(z)S_1^{\mathrm{sym}}(z) + \Omega_{-1,0}(z)N_0^{\mathrm{sym}}(z) + \Omega_{-1,-1}(z)U_{-1}^{\mathrm{sym}}(z) , \\
N_0^{\mathrm{sym}}(z) &= \Omega_{0,1}(z)S_1^{\mathrm{sym}}(z) + \Omega_{0,0}(z)N_0^{\mathrm{sym}}(z) + \Omega_{0,-1}(z)U_{-1}^{\mathrm{sym}}(z) , \\
N_1^{\mathrm{sym}}(z) &= \Omega_{1,1}(z)S_1^{\mathrm{sym}}(z) + \Omega_{1,0}(z)N_0^{\mathrm{sym}}(z) + \Omega_{1,-1}(z)U_{-1}^{\mathrm{sym}}(z) .
\end{aligned} \tag{4.15}$$

Likewise, consider the input to the system given by

$$\Phi_v^g(z) = \frac{1}{2}\left(\delta[v]\delta_{g,1} - \delta[v]\delta_{g,-1}\right) , \tag{4.16}$$

that is, we start with half unit pulses at vertex $(0,1)$ and a negative unit pulse at $(0,-1)$. Due to this initial data, the system in figure 6 is always antisymmetric with respect to a flip about the vertex $(0,0)$, which means

$$\Psi_v^g(z) = -\Psi_{-v}^{-g}(z) . \tag{4.17}$$

For this set of initial data, define

$$\begin{aligned}
S_0^{\mathrm{asym}}(z) &\equiv \Psi_0^0(z) = 0 , \\
S_1^{\mathrm{asym}}(z) &\equiv \Psi_0^1(z) = -\Psi_0^{-1}(z) , \\
N_{-1}^{\mathrm{asym}}(z) &\equiv \Psi_1^{-1}(z) = -\Psi_{-1}^1(z) , \\
N_0^{\mathrm{asym}}(z) &\equiv \Psi_1^0(z) = -\Psi_{-1}^0(z) , \\
N_1^{\mathrm{asym}}(z) &\equiv \Psi_1^1(z) = -\Psi_{-1}^{-1}(z) , \\
U_{-1}^{\mathrm{asym}}(z) &\equiv \Psi_2^{-1}(z) = -\Psi_{-2}^1(z) .
\end{aligned} \tag{4.18}$$

We can write down similar expressions for these functions using eqns. (4.2),

$$\begin{aligned} S_1^{\text{asym}}(z) &= \Omega_{1,1}(z)N_{-1}^{\text{asym}}(z) - \Omega_{1,-1}(z)N_{-1}^{\text{asym}}(z) + \frac{1}{2}\,, \\ N_{-1}^{\text{asym}}(z) &= \Omega_{-1,1}(z)S_1^{\text{asym}}(z) + \Omega_{-1,0}(z)N_0^{\text{asym}}(z) + \Omega_{-1,-1}(z)U_{-1}^{\text{asym}}(z)\,, \\ N_0^{\text{asym}}(z) &= \Omega_{0,1}(z)S_1^{\text{asym}}(z) + \Omega_{0,0}(z)N_0^{\text{asym}}(z) + \Omega_{0,-1}(z)U_{-1}^{\text{asym}}(z)\,, \\ N_1^{\text{asym}}(z) &= \Omega_{1,1}(z)S_1^{\text{asym}}(z) + \Omega_{1,0}(z)N_0^{\text{asym}}(z) + \Omega_{1,-1}(z)U_{-1}^{\text{asym}}(z)\,. \end{aligned} \tag{4.19}$$

Without extra information we cannot outright solve the systems (4.15) and (4.19), since the number of unknowns is always one less than the number of equations. However, note that, from eq. (4.10),

$$\begin{aligned} S_1^{\text{sym}}(z) &= \frac{1}{2}\left[M_{00}^{1,1}(z) + M_{00}^{1,-1}(z)\right]\,, \\ S_1^{\text{asym}}(z) &= \frac{1}{2}\left[M_{00}^{1,1}(z) - M_{00}^{1,-1}(z)\right]\,. \end{aligned} \tag{4.20}$$

Moreover, from equation (4.9),

$$M_{00}^{gh}(z) = \int_{-1/2}^{1/2} [(I - K(\xi; z))^{-1}]_{gh}\, d\xi\,. \tag{4.21}$$

For this system, the propagator takes the form

$$K(\xi; z) = \begin{bmatrix} \Omega_{-1,-1}(z)e^{-2\pi i\xi} & \Omega_{-1,0}(z) & \Omega_{-1,1}(z)e^{2\pi i\xi} \\ \Omega_{0,-1}(z)e^{-2\pi i\xi} & \Omega_{0,0}(z) & \Omega_{0,1}(z)e^{2\pi i\xi} \\ \Omega_{1,-1}(z)e^{-2\pi i\xi} & \Omega_{1,0}(z) & \Omega_{1,1}(z)e^{2\pi i\xi} \end{bmatrix}\,. \tag{4.22}$$

Computing the determinant of the matrix $I - K(\xi; z)$ gives

$$\begin{aligned} \det(I - K(\xi; z)) = &- \det K(\xi; z) + 1 - \Omega_{0,0}(z) - \Omega_{-1,1}(z)\Omega_{1,-1}(z) + \Omega_{-1,-1}(z)\Omega_{1,1}(z) \\ &+ e^{-2\pi i\xi}(-\Omega_{-1,-1}(z) - \Omega_{-1,0}(z)\Omega_{0,-1}(z) + \Omega_{-1,-1}(z)\Omega_{0,0}(z)) \\ &+ e^{2\pi i\xi}(-\Omega_{1,1}(z) - \Omega_{0,1}(z)\Omega_{1,0}(z) + \Omega_{0,0}(z)\Omega_{1,1}(z))\,. \end{aligned} \tag{4.23}$$

Since

$$\det K(\xi; z) = \det \begin{bmatrix} \Omega_{-1,-1}(z) & \Omega_{-1,0}(z) & \Omega_{-1,1}(z) \\ \Omega_{0,-1}(z) & \Omega_{0,0}(z) & \Omega_{0,1}(z) \\ \Omega_{1,-1}(z) & \Omega_{1,0}(z) & \Omega_{1,1}(z) \end{bmatrix}\,, \tag{4.24}$$

and by virtue of the symmetry condition (4.11), we can write

$$\det(I - K(\xi; z)) = D_0(z) + D_1(z)\cos(2\pi\xi)\,, \tag{4.25}$$

where $D_0(z)$ and $D_1(z)$ depend only on $z$ and are nonzero in the typical non-degenerate case, where all $\Omega_{g,h}(z)$ are nonzero except perhaps $\Omega_{1,-1}(z)$ and $\Omega_{-1,1}(z)$. If this is the case, then eq. (4.21) becomes

$$M_{00}^{gh}(z) = \int_{-1/2}^{1/2} \frac{\text{adj}(I - K(\xi; z))_{gh}}{D_0(z) + D_1(z)\cos(2\pi\xi)}\, d\xi\,, \tag{4.26}$$

where adj denotes the adjugate matrix. We can now use the same residue calculus trick that was introduced in section 3.1,

$$M_{00}^{gh}(z) = 2\pi i \sum_k \text{res}_{\xi\to\xi_k} \frac{\text{adj}(I - K(\xi; z))_{gh}}{D_0(z) + D_1(z)\cos(2\pi\xi)}\,, \tag{4.27}$$

where $\xi_k$ denote the poles of the function under in integral in eq. (4.26) in the region $-1/2 < \text{Re}[\xi] < 1/2$ and $\text{Im}[\xi] > 0$. These occur at

$$\xi_k = \frac{1}{2\pi}\cos^{-1}\left[-\frac{D_0(z)}{D_1(z)}\right]\,, \tag{4.28}$$

where the branch of $\cos^{-1}$ is chosen appropriately. Thus, we can use residue calculus to solve for $M_{00}^{1,1}(z)$ and $M_{00}^{1,-1}(z)$. Using eq. (4.20) enables us to compute $S_1^{\text{sym}}(z)$ and $S_1^{\text{asym}}(z)$, which then means the systems of equations (4.15) and (4.19) have the same number of equations as unknowns and can be solved by matrix inversion. Once this has been done, we can compute

$$\begin{aligned} N_1(z) &\equiv M_{01}^{1,1}(z) = N_1^{\text{sym}}(z) + N_1^{\text{asym}}(z)\,, \\ N_0(z) &\equiv M_{01}^{0,1}(z) = N_0^{\text{sym}}(z) + N_0^{\text{asym}}(z)\,, \\ N_{-1}(z) &\equiv M_{01}^{-1,1}(z) = N_{-1}^{\text{sym}}(z) + N_{-1}^{\text{asym}}(z)\,. \end{aligned} \tag{4.29}$$

Now, we use the same machinery we used in section 3.4. To compute $M_{N0}^{g,1}(z)$ for $N > 0$, we use the decomposition (3.54). We mark the vertices $v_i = (i, 1)$ for $0 < i < N$ with dummy variables $x_i$ and mark $v_N = (N, g)$ with the variable $x_N$. Since a walk must pass through all of the vertices $v_i$ in sequence to reach the target vertex $v_N$, the decomposition (3.54) becomes

$$M_{N,0}^{g,1}(z,x) = x_1x_2...x_N M_{N,N}^{g,g}(z,x)\left[\frac{\partial}{\partial x_N} M_{N,N-1}^{g,1}(z,x)\right]_{x_N=0} \prod_{i=1}^{N-1}\left[\frac{\partial}{\partial x_i} M_{i,i-1}^{1,1}(z,x)\right]_{x_i=0}. \tag{4.30}$$

Furthermore, setting $x_i = 1$ and using translation invariance of the system, we obtain

$$M_{N0}^{g,1}(z) = M_{NN}^{g,g}(z) R_g(z) R_1(z)^{N-1}\,, \tag{4.31}$$

where

$$R_g(z) = \frac{\partial}{\partial x_N} M_{N,N-1}^{g,1}(z, 1, ..., 1, 0)\,. \tag{4.32}$$

To compute $R^g(z)$, one can use of the expressions in (4.29), since we have

$$N^g(z) = M_{NN}^{g,g}(z) R_g(z) = M_{00}^{g,g}(z) R_g(z)\,. \tag{4.33}$$

Therefore,

$$R_g(z) = \frac{N_g(z)}{M_{00}^{g,g}(z)}\,, \tag{4.34}$$

which means

$$M_{N0}^{g,1}(z) = N_g(z)\left[\frac{N_1(z)}{M_{00}^{1,1}(z)}\right]^{N-1} = \left[N_g^{\text{sym}}(z) + N_g^{\text{asym}}(z)\right]\left[\frac{N_1^{\text{sym}}(z) + N_1^{\text{asym}}(z)}{M_{00}^{1,1}(z)}\right]^{N-1}. \tag{4.35}$$

To compute transfer functions for $N < 0$, we mark the vertices $v_i = (-i, -1)$ for $0 \le i < N$ and $v_N = (N, g)$. The decomposition (3.54) becomes

$$\begin{aligned} M_{N,0}^{g,1}(z,x) = x_1x_2...x_N M_{N,N}^{g,g}(z,x)&\left[\frac{\partial}{\partial x_N} M_{N,N+1}^{g,-1}(z,x)\right]_{x_N=0} \\ \cdot \prod_{i=1}^{N-1}&\left[\frac{\partial}{\partial x_i} M_{-i,-i+1}^{-1,-1}(z,x)\right]_{x_i=0}\left[\frac{\partial}{\partial x_0} M_{0,0}^{-1,1}(z,x)\right]_{x_0=0}. \end{aligned} \tag{4.36}$$

Once again setting $x_i = 0$ and using the translation invariance of the system, we obtain

$$M_{N,0}^{g,1}(z) = M_{N,N}^{g,g}(z) L_g(z) L_{-1}(z)^{N-1} W_{-1,1}(z)\,, \tag{4.37}$$

where

$$\begin{aligned} L_g(z) &= \frac{\partial}{\partial x_N} M_{N,N+1}^{g,-1}(z, 1, ..., 1, 0)\,, \\ W_{-1,1}(z) &= \frac{\partial}{\partial x_0} M_{0,0}^{-1,1}(z, 0, 1, ..., 1)\,. \end{aligned} \tag{4.38}$$

Computing $W_{g,h}(z)$ is fairly simple, since for $N = 0$, we should have

$$M_{00}^{-1,1}(z) = M_{00}^{g,g}(z) W_{-1,1}(z)\,, \tag{4.39}$$

hence

$$W_{-1,1}(z) = \frac{M_{00}^{-1,1}(z)}{M_{00}^{1,1}(z)}\,. \tag{4.40}$$

Furthermore,

$$M_{-1,0}^{g,1}(z) = M_{00}^{g,g}(z) L_g(z) W_{-1,1}(z)\,. \tag{4.41}$$

We note that

$$M_{-1,0}^{g,1}(z) = N_1^{\mathrm{sym}}(z) - N_1^{\mathrm{asym}}(z)\,, \tag{4.42}$$

Therefore, it follows from eq. (4.41) that

$$L_g(z) = \frac{M_{-1,0}^{g,1}(z)}{M_{0,0}^{g,g}(z) W_{-1,1}(z)}\,. \tag{4.43}$$

We conclude by subsituting this into eq. (4.37),

$$M_{N,0}^{g,1}(z) = M_{0,0}^{g,g}(z) \frac{M_{-1,0}^{g,1}(z)}{M_{0,0}^{g,g}(z) W_{-1,1}(z)} \left[\frac{M_{-1,0}^{-1,1}(z)}{M_{0,0}^{-1,-1}(z) W_{-1,1}(z)}\right]^{N-1} W_{-1,1}(z)\,, \tag{4.44}$$

and then using eq. (4.42) and eq. (4.40),

$$M_{N0}^{g,1}(z) = \left[N_g^{\mathrm{sym}}(z) - N_g^{\mathrm{asym}}(z)\right] \left[\frac{N_1^{\mathrm{sym}}(z) - N_1^{\mathrm{asym}}(z)}{M_{00}^{-1,-1}(z)}\right]^{N-1} \left[\frac{M_{00}^{1,1}(z)}{M_{00}^{-1,1}(z)}\right]^{N-1}\,. \tag{4.45}$$

Together, eqns. (4.35) and (4.45) give us all entries of form $M_{uv}^{g,1}$ and $M_{uv}^{g,-1}$ by symmetry. Entries $M_{uv}^{g,0}$ can be computed in a similar fashion.

4.2. **Propagation in a Thin Layer.** Once we have all entries of the form $M_{uv}^{g,1}$ and $M_{uv}^{g,-1}$, we can turn to examining propagation in a thin layer – the directional analogue of section 3.6. We assume that the signal enters the layer at vertex $(s,1)$ and exists the layer at vertices $(0,-1)$ and $(D,1)$ where $D$ is the depth of the layer. What exits at vertex $(0,-1)$ is the reflected signal and what exists at vertex $(D,1)$ is the transmitted signal, we call the corresponding transfer functions $H_R(z)$ and $H_T(z)$ respectively. The same technique used in section 3.6 gives us

$$\begin{bmatrix} H_R(z) \\ H_T(z) \end{bmatrix} = \begin{bmatrix} M_{00}^{-1,-1}(z) & M_{0D}^{-1,1}(z) \\ M_{D0}^{1,-1}(z) & M_{DD}^{1,1}(z) \end{bmatrix}^{-1} \begin{bmatrix} M_{0s}^{-1,1}(z) \\ M_{Ds}^{1,1}(z) \end{bmatrix}\,. \tag{4.46}$$

This equation allows us to compute $H_R(z)$ and $H_T(z)$ directly. The particular case of interest is $s = 0$, where the signal is introduced at the left end of the scattering layer. Then, the above becomes

$$\begin{bmatrix} H_R(z) \\ H_T(z) \end{bmatrix} = \begin{bmatrix} M_{00}^{-1,-1}(z) & \frac{\left[N_1^{\mathrm{sym}}(z) - N_1^{\mathrm{asym}}(z)\right]^D M_{00}^{1,1}(z)^{D-1}}{M_{00}^{-1,-1}(z)^{D-1} M_{00}^{-1,1}(z)^{D-1}} \\ \frac{\left[N_1^{\mathrm{sym}}(z) - N_1^{\mathrm{asym}}(z)\right]^D M_{00}^{1,1}(z)^{D-1}}{M_{00}^{-1,-1}(z)^{D-1} M_{00}^{-1,1}(z)^{D-1}} & M_{00}^{1,1}(z) \end{bmatrix}^{-1} \begin{bmatrix} M_{00}^{-1,1}(z) \\ \frac{N_1(z)^D}{M_{00}^{1,1}(z)^{D-1}} \end{bmatrix}, \tag{4.47}$$

where, from (4.27),

$$M_{00}^{gh}(z) = 2\pi i \sum_k \mathrm{res}_{\xi \to \xi_k} \frac{\mathrm{adj}(I - K(\xi; z))_{gh}}{D_0(z) + D_1(z)\cos(2\pi\xi)}\,, \tag{4.48}$$

and

$$N_1(z) = N_1^{\mathrm{sym}}(z) + N_1^{\mathrm{asym}}(z)\,, \tag{4.49}$$

and $N_1^{\mathrm{sym}}(z)$ and $N_1^{\mathrm{asym}}(z)$ are computed by solving the linear systems (4.15) and (4.19).

4.3. **Redundant Symmetric Grids in Dimension One.** To perform a reduction from a general case to the case of dimension one, we need to slightly modify the above structure. Suppose instead of generators $\mathcal{G} = \{-1, 0, 1\}$ we instead have generators

$$\mathcal{G} = \{-1, u_1, u_2, ..., u_k, 1\}\,, \tag{4.50}$$

where $u_1, ..., u_k$ are redundant copies of zero. We also still impose the symmetry conditions

$$\Omega_{g,h}(z) = \Omega_{-g,-h}(z)\,, \tag{4.51}$$

with the understanding that $-u_i = u_i$. An example of this sort of graph can be seen in figure 7, with $k = 2$.

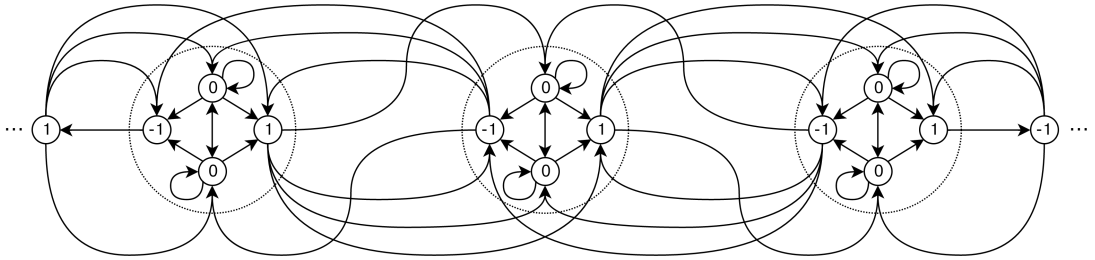


FIGURE 7. Redundant symmetric grid graph in dimension one with directional scattering, with generators $\mathcal{G} = \{-1, 0, 0, 1\}$. Note that each vertex on $\mathbb{Z}$ (denoted by dotted circles) is expanded into four individual vertices corresponding to scattering direction.

In this case, the propagator takes the form

$$K(\xi; z) = \begin{bmatrix} \Omega_{-1,-1}(z)e^{-2\pi i\xi} & \Omega_{-1,u_1}(z) & ... & \Omega_{-1,u_k}(z) & \Omega_{-1,1}(z)e^{2\pi i\xi} \\ \Omega_{u_1,-1}(z)e^{-2\pi i\xi} & \Omega_{u_1,u_1}(z) & ... & \Omega_{u_1,u_k}(z) & \Omega_{u_1,1}(z)e^{2\pi i\xi} \\ \vdots & \vdots & \ddots & \vdots & \vdots \\ \Omega_{u_k,-1}(z)e^{-2\pi i\xi} & \Omega_{u_k,u_1}(z) & ... & \Omega_{u_k,u_k}(z) & \Omega_{u_k,1}(z)e^{2\pi i\xi} \\ \Omega_{1,-1}(z)e^{-2\pi i\xi} & \Omega_{1,u_1}(z) & ... & \Omega_{1,u_k}(z) & \Omega_{1,1}(z)e^{2\pi i\xi} \end{bmatrix}. \tag{4.52}$$

With a bit of work, one can show that the determinant $\det(I - K(\xi; z))$ takes the form

$$\det(I - K(\xi; z)) = D_0(z) + D_1(z)\cos(2\pi\xi)\,, \tag{4.53}$$

due to the symmetry condition (4.51). This can be done by using induction and expansion of the determinant of $I - K(\xi; z)$ by minors along the $u_i, u_i$ diagonal elements of $I - K(\xi; z)$ and using the determinant (4.23) as a base case. Just like in the previous section (see eq. (4.27)), this gives us an expression for the matrix values $M_{00}^{gh}(z)$,

$$M_{00}^{gh}(z) = \int_{-1/2}^{1/2} \frac{\mathrm{adj}(I - K(\xi; z))_{gh}}{D_0(z) + D_1(z)\cos(2\pi\xi)}\, d\xi = 2\pi i \sum_k \mathrm{res}_{\xi\to\xi_k} \frac{\mathrm{adj}(I - K(\xi; z))_{gh}}{D_0(z) + D_1(z)\cos(2\pi\xi)}\,, \tag{4.54}$$

where $\xi_k$ are the poles of the function under the integral above in the region $-1/2 < \mathrm{Re}[\xi] < 1/2$ and $\mathrm{Im}[\xi] > 0$. Once again, these occur at

$$\xi_k = \frac{1}{2\pi}\cos^{-1}\left[-\frac{D_0(z)}{D_1(z)}\right]. \tag{4.55}$$

Now, we reuse the variables defined in (4.14) and (4.18), with slight alterations. Instead of defining $S_0^{\mathrm{sym}}$ and $S_0^{\mathrm{asym}}$, we define

$$S_{u_i}^{\mathrm{sym}}(z) \equiv \Psi_0^{u_i}(z)\,, \tag{4.56}$$

when the input to the system is given by $\Phi_v^g(z) = \frac{1}{2}\left(\delta[v]\delta_{g,1} + \delta[v]\delta_{g,-1}\right)$. And we define

$$S_{u_i}^{\text{asym}}(z) \equiv \Psi_0^{u_i}(z)\,, \tag{4.57}$$

when the input to the system is given by $\Phi_v^g(z) = \frac{1}{2}\left(\delta[v]\delta_{g,1} - \delta[v]\delta_{g,-1}\right)$. Using the symmetry of the underlying graph with respect to transformations $(v,g) \to (-v,-g)$ as we did in the previous section gives us the system of equations

$$\begin{aligned}
S_{u_i}^{\text{sym}}(z) &= \Omega_{0,1}(z)N_{-1}^{\text{sym}}(z) + \Omega_{0,-1}(z)N_{-1}^{\text{sym}}(z) + \sum_{j=1}^{k}\Omega_{u_i,u_j}(z)S_{u_j}^{\text{sym}}(z) + \frac{1}{2}\,,\\
S_1^{\text{sym}}(z) &= \Omega_{1,1}(z)N_{-1}^{\text{sym}}(z) + \Omega_{1,-1}(z)N_{-1}^{\text{sym}}(z) + \sum_{j=1}^{k}\Omega_{1,u_j}(z)S_{u_j}^{\text{sym}}(z)\,,\\
N_{-1}^{\text{sym}}(z) &= \Omega_{-1,1}(z)S_1^{\text{sym}}(z) + \sum_{j=1}^{k}\Omega_{-1,u_j}(z)N_{u_j}^{\text{sym}}(z) + \Omega_{-1,-1}(z)U_{-1}^{\text{sym}}(z)\,,\\
N_{u_i}^{\text{sym}}(z) &= \Omega_{u_i,1}(z)S_1^{\text{sym}}(z) + \sum_{j=1}^{k}\Omega_{u_i,u_j}(z)N_{u_j}^{\text{sym}}(z) + \Omega_{u_i,-1}(z)U_{-1}^{\text{sym}}(z)\,,\\
N_1^{\text{sym}}(z) &= \Omega_{1,1}(z)S_1^{\text{sym}}(z) + \sum_{j=1}^{k}\Omega_{1,u_j}(z)N_{u_j}^{\text{sym}}(z) + \Omega_{1,-1}(z)U_{-1}^{\text{sym}}(z)\,,
\end{aligned} \tag{4.58}$$

and correspondingly,

$$\begin{aligned}
S_1^{\text{asym}}(z) &= \Omega_{1,1}(z)N_{-1}^{\text{asym}}(z) - \Omega_{1,-1}(z)N_{-1}^{\text{asym}}(z) + \frac{1}{2}\,,\\
N_{-1}^{\text{asym}}(z) &= \Omega_{-1,1}(z)S_1^{\text{asym}}(z) + \sum_{j=1}^{k}\Omega_{-1,u_j}(z)N_{u_j}^{\text{asym}}(z) + \Omega_{-1,-1}(z)U_{-1}^{\text{asym}}(z)\,,\\
N_{u_i}^{\text{asym}}(z) &= \Omega_{u_i,1}(z)S_1^{\text{asym}}(z) + \sum_{j=1}^{k}\Omega_{u_i,u_j}(z)N_{u_j}^{\text{asym}}(z) + \Omega_{u_i,-1}(z)U_{-1}^{\text{asym}}(z)\,,\\
N_1^{\text{asym}}(z) &= \Omega_{1,1}(z)S_1^{\text{asym}}(z) + \sum_{j=1}^{k}\Omega_{1,u_j}(z)N_{u_j}^{\text{asym}}(z) + \Omega_{1,-1}(z)U_{-1}^{\text{asym}}(z)\,.
\end{aligned} \tag{4.59}$$

Since we know that

$$\begin{aligned}
S_1^{\text{sym}}(z) &= \frac{1}{2}\left[M_{00}^{1,1}(z) + M_{00}^{1,-1}(z)\right]\,,\\
S_1^{\text{asym}}(z) &= \frac{1}{2}\left[M_{00}^{1,1}(z) - M_{00}^{1,-1}(z)\right]\,,
\end{aligned} \tag{4.60}$$

we can solve for the remaining variables above by using the linear systems (4.58) and (4.59). Then, using the same argument we used in the previous section, for $N > 0$

$$M_{N0}^{g,1}(z) = \left[N_g^{\text{sym}}(z) + N_g^{\text{asym}}(z)\right]\left[\frac{N_1^{\text{sym}}(z) + N_1^{\text{asym}}(z)}{M_{00}^{1,1}(z)}\right]^{N-1}\,, \tag{4.61}$$

and likewise, for $N \leq 0$,

$$M_{N0}^{g,1}(z) = \left[N_g^{\text{sym}}(z) - N_g^{\text{asym}}(z)\right]\left[\frac{N_1^{\text{sym}}(z) - N_1^{\text{asym}}(z)}{M_{00}^{-1,-1}(z)}\right]^{N-1}\left[\frac{M_{00}^{1,1}(z)}{M_{00}^{-1,1}(z)}\right]^{N-1}\,. \tag{4.62}$$

Transfer functions for propagation in a thin layer of depth $D$ can then be computed exactly as we did before,

(4.63)
$$\begin{bmatrix} H_R(z) \\ H_T(z) \end{bmatrix} = \begin{bmatrix} M_{00}^{-1,-1}(z) & \frac{\left[N_1^{\rm sym}(z)-N_1^{\rm asym}(z)\right]^D M_{00}^{1,1}(z)^{D-1}}{M_{00}^{-1,-1}(z)^{D-1}M_{00}^{-1,1}(z)^{D-1}} \\ \frac{\left[N_1^{\rm sym}(z)-N_1^{\rm asym}(z)\right]^D M_{00}^{1,1}(z)^{D-1}}{M_{00}^{-1,-1}(z)^{D-1}M_{00}^{-1,1}(z)^{D-1}} & M_{00}^{1,1}(z) \end{bmatrix}^{-1} \begin{bmatrix} M_{00}^{-1,1}(z) \\ \frac{N_1(z)^D}{M_{00}^{1,1}(z)^{D-1}} \end{bmatrix},$$

where $N_1(z) = N_1^{\rm sym}(z) + N_1^{\rm asym}(z)$. Now that we've established this machinery, we can finally look at the reduction from higher dimensions to the one dimensional case.

4.4. **Reduction to Dimension One.** For our reduction to work in the directional scattering case, we require the following,

(1) *Locality*: for every $\boldsymbol{g} = (v_1, v_2, ..., v_d)$, we must have $|v_d| \leq 1$.
(2) *Single Exit/Entry*: there must exist exactly one element $\boldsymbol{g}_1 = (v_1, v_2, ..., v_d)$ in $\mathcal{G}$ with $v_d = 1$ and exactly one element $\boldsymbol{g}_{-1} = (u_1, u_2, ..., u_d)$ with $u_d = -1$.
(3) *Symmetry*: for every $\boldsymbol{g} = (v_1, v_2, ..., v_d)$ and $\boldsymbol{h} = (u_1, u_2, ..., u_d)$ in the set of generators $\mathcal{G}$, there must be corresponding generators $\boldsymbol{g}' = (v_1, v_2, ..., -v_d)$ and $\boldsymbol{h}' = (u_1, u_2, ..., -u_d)$ in $\mathcal{G}$. Moreover, $\Omega_{\boldsymbol{g},\boldsymbol{h}}(z) = \Omega_{\boldsymbol{g}',\boldsymbol{h}'}(z)$.

The collapse procedure is done as follows. Consider the propagation of a $d-1$-dimensional plane wave on $G$, that is, with input signal

$$\Phi^{\boldsymbol{g}}_{(v_1,v_2,...,v_{d-1},v_d)}(z) = e^{2\pi i \Xi_1 v_1} e^{2\pi i \Xi_2 v_2} ... e^{2\pi i \Xi_{d-1} v_{d-1}} \delta[v_d] \delta_{\boldsymbol{g},\boldsymbol{g}_1} \,. \tag{4.64}$$

This initial data is a plane wave entering the scattering region at $v_d = 0$ and moving to the right. If we define

$$\Omega_{\boldsymbol{g}\boldsymbol{h}}(\xi_1, ..., \xi_{d-1}; z) \equiv \Omega_{\boldsymbol{g}\boldsymbol{h}}(z) \prod_{i=j}^{d-1} e^{2\pi i h_j \xi_j} \,, \tag{4.65}$$

and enumerate the elements of $\mathcal{G}^0 \equiv \mathcal{G} \setminus \{\boldsymbol{g}_1, \boldsymbol{g}_{-1}\}$ as $\boldsymbol{u}_1, \boldsymbol{u}_2, ..., \boldsymbol{u}_k$, then the propagator can be written as

(4.66)
$$K(\boldsymbol{\xi}; z) = \begin{bmatrix} \Omega_{\boldsymbol{g}_{-1},\boldsymbol{g}_{-1}}(\boldsymbol{\xi}; z) e^{-2\pi i \xi_d} & \Omega_{\boldsymbol{g}_{-1},\boldsymbol{u}_1}(\boldsymbol{\xi}; z) & ... & \Omega_{\boldsymbol{g}_{-1},\boldsymbol{u}_k}(\boldsymbol{\xi}; z) & \Omega_{\boldsymbol{g}_{-1},\boldsymbol{g}_1}(\boldsymbol{\xi}; z) e^{2\pi i \xi_d} \\ \Omega_{\boldsymbol{u}_1,\boldsymbol{g}_{-1}}(\boldsymbol{\xi}; z) e^{-2\pi i \xi_d} & \Omega_{\boldsymbol{u}_1,\boldsymbol{u}_1}(\boldsymbol{\xi}; z) & ... & \Omega_{\boldsymbol{u}_1,\boldsymbol{u}_k}(\boldsymbol{\xi}; z) & \Omega_{\boldsymbol{u}_1,\boldsymbol{g}_1}(\boldsymbol{\xi}; z) e^{2\pi i \xi_d} \\ \vdots & \vdots & \ddots & \vdots & \vdots \\ \Omega_{\boldsymbol{u}_k,\boldsymbol{g}_{-1}}(\boldsymbol{\xi}; z) e^{-2\pi i \xi_d} & \Omega_{\boldsymbol{u}_k,\boldsymbol{u}_1}(\boldsymbol{\xi}; z) & ... & \Omega_{\boldsymbol{u}_k,\boldsymbol{u}_k}(\boldsymbol{\xi}; z) & \Omega_{\boldsymbol{u}_k,\boldsymbol{g}_1}(\boldsymbol{\xi}; z) e^{2\pi i \xi_d} \\ \Omega_{\boldsymbol{g}_1,\boldsymbol{g}_{-1}}(\boldsymbol{\xi}; z) e^{-2\pi i \xi_d} & \Omega_{\boldsymbol{g}_1,\boldsymbol{u}_1}(\boldsymbol{\xi}; z) & ... & \Omega_{\boldsymbol{g}_1,\boldsymbol{u}_k}(\boldsymbol{\xi}; z) & \Omega_{\boldsymbol{g}_1,\boldsymbol{g}_1}(\boldsymbol{\xi}; z) e^{2\pi i \xi_d} \end{bmatrix}.$$

Note the similarity of this propagator to the propagator (4.52) from the previous section.

The Fourier transform of the input data is

$$\hat{\Phi}^{\boldsymbol{g}}(\xi_1, ..., \xi_d; z) = \delta[\xi_1 - \Xi_1] ... \delta[\xi_{d-1} - \Xi_{d-1}] \, \delta_{\boldsymbol{g},\boldsymbol{g}_1} \,. \tag{4.67}$$

From eq. (4.8), we have

$$\begin{aligned} \Psi^{\boldsymbol{g}}_{\boldsymbol{v}}(\boldsymbol{\xi}; z) &= \int_{-1/2}^{1/2} e^{2\pi i \boldsymbol{\xi}\cdot\boldsymbol{v}} (I - K(\boldsymbol{\xi}; z))^{-1} \hat{\Phi}(\boldsymbol{\xi}; z) \, d\boldsymbol{\xi} \\ &= \prod_{i=j}^{d-1} e^{2\pi i v_j \Xi_j} \left[ \int_{-1/2}^{1/2} e^{2\pi i \xi v_d} (I - K(\Xi_1, ..., \Xi_{d-1}, \xi; z))^{-1} \, d\xi \right]_{\boldsymbol{g},\boldsymbol{g}_1} . \end{aligned} \tag{4.68}$$

Defining

$$\zeta^{\boldsymbol{g}}_v(\Xi_1, ..., \Xi_{d-1}; z) \equiv \left[ \int_{-1/2}^{1/2} e^{2\pi i \xi v} (I - K(\Xi_1, ..., \Xi_{d-1}, \xi; z))^{-1} \, d\xi \right]_{\boldsymbol{g},\boldsymbol{g}_1} , \tag{4.69}$$

we can see that the solution of $\zeta_v^{\boldsymbol{g}}(\Xi_1, ..., \Xi_{d-1}; z)$ on the above graph is equivalent to $M_{0,v}^{\boldsymbol{g},1}(z)$ on the graph studied in the previous section 4.3 (see the propagator 4.52), with

$$\Omega_{\boldsymbol{gh}}(z) \equiv \Omega_{\boldsymbol{gh}}(\Xi_1, ..., \Xi_{d-1}; z)\,. \tag{4.70}$$

Hence, $\zeta_v^{\boldsymbol{g}}(\Xi_1, ..., \Xi_{d-1}; z)$ can be computed using the techniques of section 4.3. Once this has been done, transfer functions for propagation in a thin layer can be computed using the expression (4.63).

## Appendix A. Propagation Graph Models with Random Transfer Functions

A.1. **Unit Delay with Constant Real Attenuation.** To begin, we consider the case where $A$ is simply the adjacency matrix of an Erdös-Réyni random graph multiplied by a scalar $\alpha$,

$$A \equiv \alpha(n) \begin{bmatrix} 0 & X_{12} & X_{13} & \dots & X_{1n} \\ \star & 0 & X_{23} & \dots & X_{2n} \\ \star & \star & 0 & \dots & X_{3n} \\ \vdots & \vdots & \vdots & \ddots & \vdots \\ \star & \star & \star & \dots & 0 \end{bmatrix}, \tag{A.1}$$

where $\star$ denotes symmetric matrix entries, and $X_{ij}$ are i.i.d. Bernoulli random variables,

$$X_{ij} = \begin{cases} 1 & : \text{ with probability } p \\ 0 & : \text{ with probability } 1-p \end{cases}. \tag{A.2}$$

From the previous section, we have

$$T(z) = z^{-1}A\,. \tag{A.3}$$

Systems with edge transfer matrices of the form (A.3) have impulse responses of the form

$$h[t] \equiv [z^{-t}](I - T(z))^{-1} = A^t\,, \tag{A.4}$$

where $h_{ij}[t]$ is the signal at node $i$ at time $t$ if a Dirac delta impulse $\delta[t]$ is introduced at vertex $j$. If we use the spectral decomposition of $A$, we can write

$$h_{ij}[t] = \sum_k \Lambda_{ik}\Lambda^*_{jk}\lambda_k^t\,, \tag{A.5}$$

where the $i$th column of the matrix $\Lambda$ is the $i$th eigenvector of $A$. From theorem (B.1), we know w.h.p. that $\rho(A)$ can be approximated in $O(\alpha(n)/\sqrt{n})$ as

$$\rho(A) \sim \mathcal{N}\left(\alpha(n)(np - 2p + 1), 2\alpha(n)^2p^2(1-p^2)\right)\,. \tag{A.6}$$

A.1.1. *Stability.* In particular, if $\alpha(n) = O(1/np)$, then the probability distribution (A.6) converges to a definite value, given by

$$\rho(A) \to \lim_{n\to\infty} \alpha(n)(np - 2p + 1)\,. \tag{A.7}$$

So, if $\alpha(n) = o(1/np)$,

$$\rho(A) \to 0\,. \tag{A.8}$$

And if $\alpha(n) \sim 1/np$, then

$$\rho(A) \to \beta\,, \tag{A.9}$$

where

$$\beta = \lim_{n\to\infty} \alpha(n)np\,. \tag{A.10}$$

Otherwise, if $\alpha = \omega(1/np)$, we have

$$\rho(A) \to \infty\,. \tag{A.11}$$

Moreover, if the event $\rho(A) < 1$ happens, then all the poles of the transfer matrix (2.15) lie strictly within the unit circle, and hence the impulse response $h_{ij}[t]$ has finite energy by Parseval's identity,

$$\sum_{t=0}^{\infty} |h_{ij}[t]|^2 = \int_0^1 |M_{ij}(e^{2\pi ix})|^2\,dx < \infty\,. \tag{A.12}$$

Thus, if $\lim_{n\to\infty}\alpha(n)np < 1$, the system given by (A.1) is BIBO stable w.h.p. On the other hand, if $\lim_{n\to\infty}\alpha(n)np \geq 1$, the system is unstable w.h.p., since it will have a pole on or within the unit circle.

A.1.2. *Impulse Response.* Now, we consider what the impulse responses of systems of the form (A.1) look like. We can get a pretty good idea. It is here where we use the fact that the expectation of the matrix (A.1) is nonzero and the resulting spectral gap. We can separate terms in (A.5), yielding

$$h_{ij}[t] = \Lambda_{i1}\Lambda_{j1}^{*}\lambda_1^t + \sum_{k>1}\Lambda_{ik}\Lambda_{jk}^{*}\lambda_k^t \,. \tag{A.13}$$

Furthermore, the eigenvector corresponding to $\lambda_1$ is close to the vector $\vec{1}/\sqrt{n}$. (see appendix B.1). Hence, we can reasonably assume that the term $\Lambda_{i1}\Lambda_{j1}^{*}$ will be nonzero. In fact, it should be close to 1. Therefore, if we define the error term,

$$\epsilon[t] \equiv \sum_{k>1}\Lambda_{ik}\Lambda_{jk}^{*}\lambda_k^t \,, \tag{A.14}$$

the impulse response can be then be written as

$$h_{ij}[t] = \Lambda_{i1}\Lambda_{j1}^{*}\lambda_1^t + \epsilon[t] \,. \tag{A.15}$$

Asymptotically, we expect the $\Lambda_{i1}\Lambda_{j1}^{*}\lambda_1^t$ to dominate the impulse response (A.13). However, we would also like to know how quickly this happens in practice. That is, we would like an idea of the behavior of the quantity

$$a[t] = \frac{|\epsilon[t]|}{|\Lambda_{i1}\Lambda_{j1}^{*}\lambda_1^t|} = \frac{1}{|\Lambda_{i1}\Lambda_{j1}^{*}\lambda_1^t|}\left|\sum_{k>1}\Lambda_{ik}\Lambda_{jk}^{*}\lambda_k^t\right| \,. \tag{A.16}$$

This quantity tells us at what point the error term $\epsilon[t]$ becomes negligible. To do this, consider the operator

$$B = \Lambda\left[\bigoplus_{k>1}\lambda_k\right]\Lambda^{\dagger} \,. \tag{A.17}$$

This operator is $A$ with the $\lambda_1$ spectral component removed. By theorem (B.2), w.h.p.,

$$\|B\| = |\lambda_2| < 2\alpha(n)\sqrt{p(1-p)}\sqrt{n} + O(\alpha(n)n^{1/3}\log n) \,. \tag{A.18}$$

But, we also have

$$\sum_{k>1}\Lambda_{ik}\Lambda_{jk}^{*}\lambda_k^t = \delta_i^T B^t \delta_j \,. \tag{A.19}$$

And therefore,

$$\left|\sum_{k>1}\Lambda_{ik}\Lambda_{jk}^{*}\lambda_k^t\right| \leq |\lambda_2|^t < \left[2\alpha(n)\sqrt{p(1-p)}\sqrt{n} + O(\alpha(n)n^{1/3}\log n)\right]^t \,. \tag{A.20}$$

Meanwhile, we know that $h_{ij}[0] = \delta_{ij}$. By (A.13), this tells us that

$$\begin{aligned} a[t] &< \frac{1}{|\Lambda_{i1}\Lambda_{j1}^{*}|}\left[\frac{2\alpha(n)\sqrt{p(1-p)}\sqrt{n} + O(\alpha(n)n^{1/3}\log n)}{\alpha(n)(np-2p+1)+O(\alpha(n))}\right]^t \\ &= \frac{1}{|\Lambda_{i1}\Lambda_{j1}^{*}|}\left[\frac{2\sqrt{p(1-p)}\sqrt{n} + O(n^{1/3}\log n)}{(np-2p+1)+O(1)}\right]^t \,. \end{aligned} \tag{A.21}$$

For large $n$ and small $t$, roughly

$$a[t] \lessapprox \frac{1}{|\Lambda_{i1}\Lambda_{j1}^{*}|}\left[2\sqrt{\frac{1-p}{n}}\right]^t \,. \tag{A.22}$$

Remember that the first eigenvector is close to the vector $\vec{1}/\sqrt{n}$. So, we make the approximation

$$|\Lambda_{i1}\Lambda_{j1}^{*}| \approx \frac{1}{n} \,, \tag{A.23}$$

which gives us our final approximate bound for $a[t]$,

$$a[t] \lessapprox n \left[ 2\sqrt{\frac{1-p}{n}} \right]^t . \tag{A.24}$$

This means, for large $n$ and for $t \geq 3$, we are nearly guaranteed $a[t] \ll 1$ and therefore, the error $\epsilon[t]$ becomes negligible. This bound seems to agree with numerical experiments, as seen in figures (8) and (9). In these figures, we can see the impulse response $h_{ij}[t]$ (where $i \neq j$) very quickly becomes an exponential after an initial period of silence, which lasts 2 units of time, and then a small amount of oscillation, which lasts another 3 units of time.

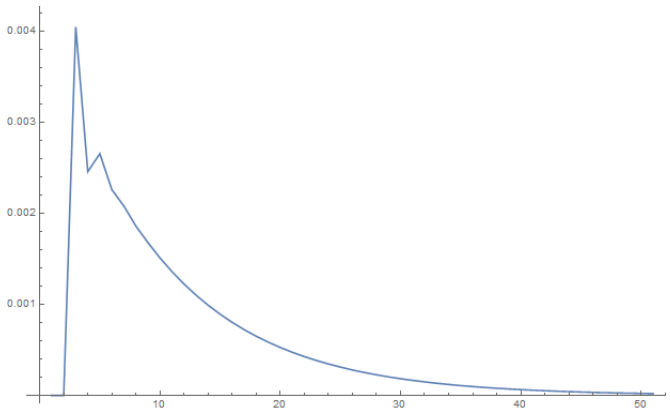


FIGURE 8. Example impulse response $h_{ij}[t]$ of system (A.1) for $\alpha = \epsilon/np$ with $\epsilon = 0.9$, $p = 0.15$, and $n = 200$

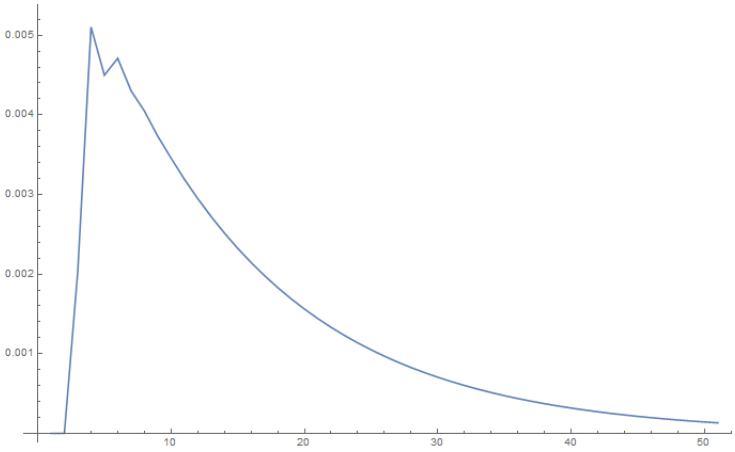


FIGURE 9. Example impulse response $h_{ij}[t]$ of system (A.1) for $\alpha = \epsilon/np$ with $\epsilon = 0.9$, $p = 0.15$, and $n = 200$

A.2. **Unit Delay with Bounded Random Real Attenuation.** This section is simply a generalization of the previous section. Here, the variables $X_{ij}$'s may have any distribution as long as the agree with the requirements of theorem (B.1).

A.2.1. *Stability.* We know

$$\rho(A) \to \lim_{n\to\infty} \alpha(n) n\mu \,, \tag{A.25}$$

where $\mu = \mathbb{E}[X_{ij}]$. Therefore, the system is stable w.h.p. if the quantity above is less than 1, and unstable otherwise.

A.2.2. *Impulse Response.* The impulse response still has the form

$$h_{ij}[t] = \Lambda_{i1}\Lambda_{j1}^{*}\lambda_1^t + \epsilon[t] \,. \tag{A.26}$$

And like before, with $\sigma = \sqrt{\mathrm{Var}[X_{ij}]}$, we have

$$a[t] \equiv \frac{|\epsilon[t]|}{|\Lambda_{i1}\Lambda_{j1}^{*}\lambda_1^t|} < \frac{1}{|\Lambda_{i1}\Lambda_{j1}^{*}|}\left[\frac{2\sigma\sqrt{n} + O(n^{1/3}\log n)}{(n-1)\mu + \sigma^2/\mu + O(1)}\right]^t \,, \tag{A.27}$$

leading to the approximation

$$a[t] \lessapprox n\left[\frac{2\sigma}{\mu\sqrt{n}}\right]^t \,. \tag{A.28}$$

Once again, for large $n$, we expect $\epsilon[t]$ to be small compared to $\Lambda_{i1}\Lambda_{j1}^{*}\lambda_1^t$ for $t \geq 3$.

A.3. **Unit Delay with Random Phase Attenuation.** Our original hope was to use this framework to model the propagation of light through a scattering medium. In such a model, we are interested in interference effects. To add these effects to the above model, we consider complex-valued signals instead of real valued ones. Furthermore, we suppose that the signals pick up random phase terms as they propagate along edges.

A.3.1. *Symmetric Case.* If we want our process to be reversible, then our matrix $A$ becomes

$$A \equiv \alpha(n)\begin{bmatrix} 0 & X_{12}e^{i\phi_{12}} & X_{13}e^{i\phi_{13}} & \dots & X_{1n}e^{i\phi_{1n}} \\ \star & 0 & X_{23}e^{i\phi_{23}} & \dots & X_{2n}e^{i\phi_{2n}} \\ \star & \star & 0 & \dots & X_{3n}e^{i\phi_{3n}} \\ \vdots & \vdots & \vdots & \ddots & \vdots \\ \star & \star & \star & \dots & 0 \end{bmatrix} \,, \tag{A.29}$$

where $\star$ now denotes conjugate symmetric entries, the $X_{ij}$ are i.i.d. Bernoulli random variables of the form (A.2), and the $\phi_{ij}$ are i.i.d. uniform random variables in $[0, 2\pi]$. Eq. (A.29) essentially adds a random phase term to the matrix in (A.1). Our first order of business is to look at the expectation of $A^t$, since it is relatively easy to compute. We have

$$\mathbb{E}[A_{ij}^t] = \alpha(n)^t \sum_{i\to j} \mathbb{E}\left[X_{il_1}...X_{l_{t-2}j}\exp\left(i\phi_{il_1} + ... + i\phi_{l_{t-2}j}\right)\right] \,, \tag{A.30}$$

where the sum denotes the sum over all walks $il_1...l_{t-2}j$ from $i$ to $j$ of length $t$ in $K_n$. Rewriting eq. (A.30),

$$\mathbb{E}[A_{ij}^t] = \alpha(n)^t \sum_{i\to j}\prod_{k<r} \mathbb{E}\left[X_{kr}^{m_{kr}+m_{rk}}\right]\mathbb{E}\left[\exp\left((m_{kr}-m_{rk})i\phi_{kr}\right)\right] \,, \tag{A.31}$$

where $m_{kr}$ is the number of times the edge $(m, r)$ appears in the path. We note that, unless $m_{kr} - m_{rk} = 0$, the $\mathbb{E}\left[\exp\left((m_{kr}-m_{rk})i\phi_{kr}\right)\right]$ term is zero. Note that at least one of these terms must be zero if $i \neq j$, due to the fact that $i$ must have one more exiting edge than entering edge. Therefore, the non-diagonal terms of $A_{ij}^t$ for $t > 0$ are expected to be zero.

Matrices of the form (A.29) are Hermitian Wigner matrices with entries satisfying

$$\mathbb{E}[|X_{ij}e^{i\phi_{ij}}|^2] = p \,. \tag{A.32}$$

Therefore, we know that the spectral radius converges asymptotically to

$$\rho(A) \to \lim_{n\to\infty} 2\alpha(n)\sqrt{np} \,. \tag{A.33}$$

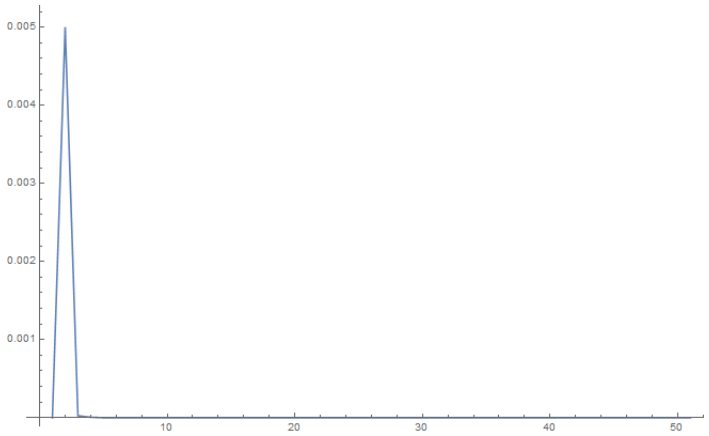


FIGURE 10. Example impulse response of system (A.29) for $\alpha = 1/np$ with , $p = 0.1$, and $n = 200$. Since we are far below the stability threshold, the response very quickly tapers off after $t = 1$.

Hence, the system is asymptotically stable if

$$\lim_{n\to\infty} 2\alpha(n)\sqrt{np} < 1\,, \tag{A.34}$$

and unstable otherwise. Furthermore, the expression (A.5) for the impulse response of the system still holds true and we have, for $t > 0$,

$$h_{ij}[t] = \sum_k \Lambda_{ik}\Lambda^*_{jk}\lambda_k^t\,. \tag{A.35}$$

For large $n$, the operator norm of the matrix $A$ is given by approximately $2\alpha(n)\sqrt{np}$. Therefore, we can state approximately that

$$|h_{ij}[t]| \lessapprox (2\alpha(n)\sqrt{np})^t\,. \tag{A.36}$$

In particular, if $\alpha(n)$ is approximately $1/np$ like the stability threshold in the previous scenario we examined, and $n$ is large, then we will get

$$h_{ij}[t] \approx 0\,. \tag{A.37}$$

On the other hand, if $\alpha(n)$ is close to the stability threshold $1/2\sqrt{np}$, then it is more difficult to give an idea of what the system will do. Since there is no spectral gap like the previous scenario, the proximity of the eigenvalues will cause the system to oscillate for a considerable amount of time until it exhibits exponential growth or decay in the large time limit, as seen in figures (11) and (12).

The figures show the absolute values of the impulse responses. We remark that the oscillation present is very structured, a result of the asymptotic semicircle eigenvalue distribution of the matrix $A$. Because the distribution is a semicircle, there are relatively few outer eigenvalues, these tend to dominate as $t$ grows large and produce this oscillation due to interference between the $\Lambda_{ik}\Lambda^*_{jk}$ coefficients.

A.3.2. *Asymmetric Case.* In the asymmetric case, we drop the assumption that our system is reversible and matrix $A$ becomes

$$A \equiv \alpha(n)\begin{bmatrix} 0 & X_{12}e^{i\phi_{12}} & X_{13}e^{i\phi_{13}} & \dots & X_{1n}e^{i\phi_{1n}} \\ X_{21}e^{i\phi_{21}} & 0 & X_{23}e^{i\phi_{23}} & \dots & X_{2n}e^{i\phi_{2n}} \\ X_{31}e^{i\phi_{31}} & X_{32}e^{i\phi_{32}} & 0 & \dots & X_{3n}e^{i\phi_{3n}} \\ \vdots & \vdots & \vdots & \ddots & \vdots \\ X_{n1}e^{i\phi_{n1}} & X_{n2}e^{i\phi_{n2}} & X_{n3}e^{i\phi_{n3}} & \dots & 0 \end{bmatrix}, \tag{A.38}$$

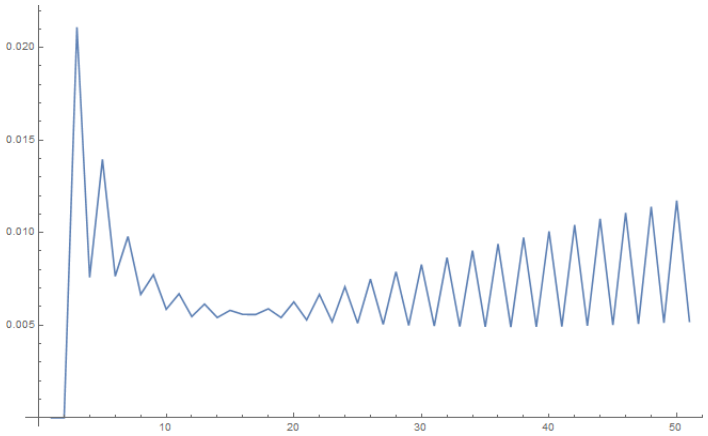


FIGURE 11. Example impulse response amplitude $|h_{ij}[t]|$ of system (A.29) at the stability threshold $\alpha = 1/2\sqrt{np}$ with , $p = 0.1$, and $n = 200$.

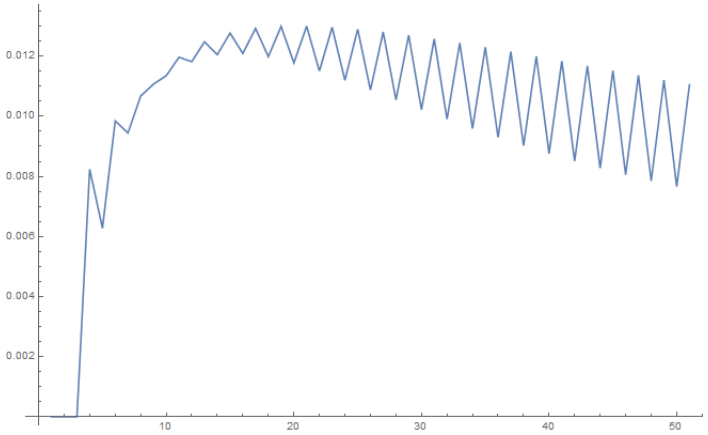


FIGURE 12. Example impulse response amplitude $|h_{ij}[t]|$ of system (A.29) at the stability threshold $\alpha = 1/2\sqrt{np}$ with , $p = 0.1$, and $n = 200$.

where the $X_{ij}$'s and $\phi_{ij}$'s are all independent and distributed as in the previous scenario (A.29), except the matrix $A$ is no longer forced to be Hermitian. The same analysis as in the previous section will show that $\mathbb{E}[A^t] = 0$ for any $t > 0$. Notice the diagonal terms also have expectation zero. This is because the system is no longer reversible, so signals can no longer back-propagate through edges as they did before. Furthermore, as long as $\alpha(n) = o(1)$, then asymptotically, $A$ has the same spectral radius as the matrix

$$B \equiv \alpha(n) \begin{bmatrix} X_{11}e^{i\phi_{11}} & X_{12}e^{i\phi_{12}} & X_{13}e^{i\phi_{13}} & \dots & X_{1n}e^{i\phi_{1n}} \\ X_{21}e^{i\phi_{21}} & X_{22}e^{i\phi_{22}} & X_{23}e^{i\phi_{23}} & \dots & X_{2n}e^{i\phi_{2n}} \\ X_{31}e^{i\phi_{31}} & X_{32}e^{i\phi_{32}} & X_{33}e^{i\phi_{33}} & \dots & X_{3n}e^{i\phi_{3n}} \\ \vdots & \vdots & \vdots & \ddots & \vdots \\ X_{n1}e^{i\phi_{n1}} & X_{n2}e^{i\phi_{n2}} & X_{n3}e^{i\phi_{n3}} & \dots & X_{nn}e^{i\phi_{nn}} \end{bmatrix}. \tag{A.39}$$

The difference between $A$ and $B$ is a diagonal matrix whose spectral radius is bounded by $\alpha(n)$. Therefore, in the large $n$ limit, we have

$$\rho(A) = \rho(B) + o(1)\,. \tag{A.40}$$

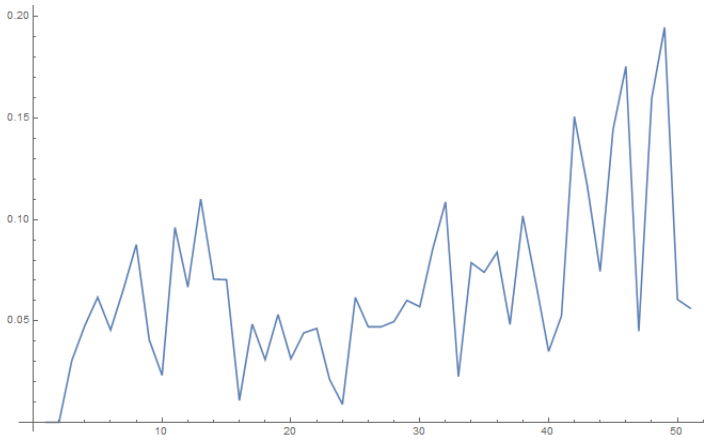


FIGURE 13. Example impulse response amplitude $|h_{ij}[t]|$ of system (A.38) at the stability threshold $\alpha = 1/\sqrt{np}$ with , $p = 0.1$, and $n = 200$.

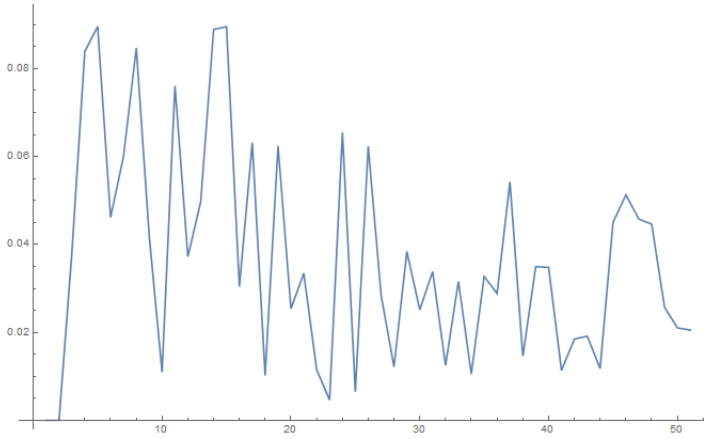


FIGURE 14. Example impulse response amplitude $|h_{ij}[t]|$ of system (A.38) at the stability threshold $\alpha = 1/\sqrt{np}$ with , $p = 0.1$, and $n = 200$.

Moreover, theorem (B.5) tells us the spectral radius of $B$. We have

$$\rho(B) \to \lim_{n\to\infty} \alpha(n)\sqrt{np}\,. \tag{A.41}$$

Hence, the same holds for $\rho(A)$. Curiously, the stability threshold for system (A.38) is therefore twice that of system (A.29). This system is asymptotically stable if

$$\lim_{n\to\infty} \alpha(n)\sqrt{np} < 1\,. \tag{A.42}$$

For large $n$, the operator norm of the matrix $A$ is approximately given by $\alpha(n)\sqrt{np}$. We can state approximately that

$$|h_{ij}[t]| \lesssim (\alpha(n)\sqrt{np})^t\,. \tag{A.43}$$

For $\alpha(n) \approx 1/np$, the system behaves more or less like the system from the previous section. When $\alpha(n)$ gets closer to the stability threshold, we again expect wild oscillation, as seen in figures (13) and (14).

The difference in the oscillation of system (A.38) seen in these figures and of system (A.29) seen in figures (11) and (12) is due to the fact that the asymptotic distribution of the eigenvalues of

(A.38) is uniform on the unit circle. Therefore, there are comparatively more eigenvalues located at the fringes of the spectrum, causing more erratic oscillation.

## Appendix B. Spectra of Large Dimensional Random Matrices

The primary tool in the analysis of random discrete-time propagation graphs is the spectra of random matrices. Fortunately, the topic of random matrix spectra is well-studied in the probability theory literature. For a large number of expectation zero matrices with i.i.d. entries, both the asymptotic distribution of eigenvalues and the asymptotic spectral radius as the dimension approaches infinity are known. Knowledge of these two factors allows us to make predictions in some cases about the properties of the transfer matrix $M(z)$.

The two crucially important properties for us are the *spectral radius* of a square random matrix $A$,

$$\rho(A) = \max_i |\lambda_i(A)|\,, \tag{B.1}$$

and the asymptotic distribution of the eigenvalues of $A$,

$$\mu_A = \lim_{n\to\infty} \frac{1}{n} \sum_i \delta_{\lambda_i}\,, \tag{B.2}$$

where $n$ is the dimension of $A$, and the $\delta_{\lambda_i}$ denote the distribution of the individual eigenvalues. In many of the cases we are interested in, the distribution $\mu_A$ is either an interval centered at zero on the real line with semicircle density, or a circle centered at zero in the complex plane with uniform density. The phenomenon of the former asymptotic distribution is commonly known as *Wigner's Semicircle Law*.

### B.1. Bounded Real Symmetric Ensembles.

Suppose we have a symmetric real random matrix $A$, whose entries are independent, but not necessarily identically distributed. Furthermore, Suppose:

(1) The entries are all bounded by some constant $B$, that is $|A_{ij}| \leq B$ for all $i$ and $j$.
(2) The nondiagonal entries share the same expectation, $\mathbb{E}[A_{ij}] = \mu$ for $i \neq j$.
(3) The nondiagonal entries share the same variance, $\mathrm{Var}[A_{ij}] = \sigma^2$ for $i \neq j$.
(4) The diagonal entries share the same expectation, $\mathbb{E}[A_{ii}] = \nu$.

Then, we have the following theorems from [6]:

**Theorem B.1.** *(Füredi, János) If $\mu = 0$, we have w.h.p.:*

$$\rho(A) = 2\sigma\sqrt{n} + O(n^{1/3}\log n)$$

**Theorem B.2.** *(Füredi, János) If $\mu > 0$ then $\rho(A)$ can be approximated in $O(1/\sqrt{n})$ by:*

$$\rho(A) \sim \mathcal{N}\left((n-1)\mu + \nu + \frac{\sigma^2}{\mu}, 2\sigma^2\right)$$

*Furthermore, w.h.p.:*

$$\max_{i\geq 2} |\lambda_i(A)| < 2\sigma\sqrt{n} + O(n^{1/3}\log n)$$

Moreover, we know from the Semicircle law that:

**Theorem B.3.** *(Semicircle Law) The asymptotic distribution $\mu_M$ of the matrix $M = \frac{1}{2\sigma\sqrt{n}}A$ is given by a Wigner semicircle distribution on the interval $(-1, 1)$.*

The class of matrices which satisfy conditions (1) through (4) includes a particular class of matrices we are interested in, namely, the adjacency matrices of random Erdös-Rényi graphs. However, one thing the reader should note is the presence of a *spectral gap* when $\mu > 0$. When the nondiagonal entries of the matrix are not centered, a significant gap appears in the spectrum of the random

matrix between the first and remaining eigenvalues, as we see in theorem (B.2). Informally, the reason for this gap becomes clear if we write the matrix $A$ as the sum:

$$A = B + \mathbb{E}[A]$$

Where $B = A - \mathbb{E}[A]$ is the random matrix which results from centering $A$. Then the all-ones vector $\vec{1}$ is an eigenvalue of $\mathbb{E}[A]$ with eigenvalue $(n-1)\mu + \nu$. Moreover, by (B.1), $\|B\| \leq 2\sigma\sqrt{n} + O(n^{1/3}\log n)$. And, by the triangle inequality:

$$\rho(A) = \|A\| \geq \|\mathbb{E}[A]\| - \|B\| \geq (n-1)\mu + \nu - 2\sigma\sqrt{n} - O(n^{1/3}\log n) \sim n\mu$$

The large first eigenvalue comes from an eigenvector which is close to the vector $\vec{1}$. The remaining eigenvectors $v_i$ are therefore nearly orthogonal to $\vec{1}$, so $Av = (B + \mathbb{E}[A])v \approx Bv$, and theorem (B.1) then limits how large the remaining eigenvalues can be.

Moreover, it is also possible to show that the eigenvalues of $A$ are concentrated about their medians by using Talagrind's Inequality [11].

B.2. **Hermitian Wigner Ensembles.** Hermitian Wigner matrices are similar to the above ensembles, except non-diagonal entries are allowed to be complex. More specifically, they must satisfy the following conditions:

(1) $\mathbb{E}[(A_{ii}^+)^2] < \infty$, where $A_{ii}^+ = \max(A_{ii}, 0)$.
(2) $\mathbb{E}[A_{ij}] = 0$ for $i \neq j$.
(3) $\mathbb{E}[|A_{ij}|^2] = \sigma^2$ for $i \neq j$.
(4) $\mathbb{E}[|A_{ij}|^4] < \infty$ for $i \neq j$.

Then from theorem (5.1) in [8]:

**Theorem B.4.** *The largest eigenvalue of $\frac{1}{\sqrt{n}}A$ tends to $2\sigma$ as $n \to \infty$ with probability 1.*

Practically, this means $\rho(A) \to 2\sigma$ as $n$ becomes very large. Furthermore, Hermitian Wigner matrices share their asymptotic eigenvalue distribution with the ensembles in the previous section, as $n \to \infty$, the distribution converges to a semicircle.

B.3. **Complex Asymmetric Ensembles with Symmetric Distribution.** Another class of matrices we are interested in are those where all entries of $A$ are i.i.d. complex random variables with:

(1) The distribution of $A_{ij}$ is symmetric, i.e. $A_{ij} = -A_{ij}$.
(2) $\mathbb{E}[A_{ij}] = 0$.
(3) $\mathbb{E}[|A_{ij}|^2] = 1$.
(4) $\mathbb{E}[|A_{ij}|^{2+\epsilon}|] < \infty$ for some $\epsilon > 0$

Then, from [9]:

**Theorem B.5.** *In probability,*

$$\lim_{n\to\infty} \frac{\rho(A)}{\sqrt{n}} = 1$$

**Theorem B.6.** *For any $\epsilon, \delta > 0$ and $B > 0$, there exists a constant $C = C(\epsilon, \delta, B) > 0$ such that for any $n \in \mathbb{N}$, where $\mathbb{E}[|A_{ij}|^{2+\epsilon}] \leq B$, we have:*

$$\mathbb{P}(\rho(A) \geq (1+\delta)\sqrt{n}) \leq \frac{C}{(\log n)^2}$$

Furthermore, we have the circle law:

**Theorem B.7.** *(Circle Law) The asymptotic distribution $\mu_M$ of the matrix $M = \frac{1}{\sqrt{n}}A$ is given by a uniform distribution on the unit circle.*

## References


1. Katz, Ori et al. "Non-invasive single-shot imaging through scattering layers and around corners via speckle correlations." *Nature photonics* 8.10 (2014): 784-790.
2. Bertolotti, Jacopo et al. "Non-invasive imaging through opaque scattering layers." *Nature* 491.7423 (2012): 232-234.
3. T. Pedersen, et al. "Modeling of reverberant radio channels using propagation graphs." *IEEE Transactions on Antennas and Propagation* 60.12 (2012): 5978-5988.
4. V. Vu. "Spectral norm of random matrices." *Proceedings of the thirty-seventh annual ACM symposium on Theory of computing* 22 May. 2005: 423-430.
5. M. Krivelevich, et al. "Approximating the independence number and the chromatic number in expected polynomial time." *Journal of combinatorial optimization* 6.2 (2002): 143-155.
6. Z. Füredi, K. János. "The eigenvalues of random symmetric matrices." *Combinatorica* 1.3 (1981): 233-241.
7. U. Haagerup, et al. "Random matrices with complex Gaussian entries." *Expositiones Mathematicae* 21.4 (2003): 293-337.
8. Z. Bai, J. W. Silverstein. *Spectral analysis of large dimensional random matrices*. New York: Springer, 2010.
9. C. Bordenave, et al. "On the spectral radius of a random matrix." *arXiv preprint* arXiv:1607.05484 (2016).
10. S. Geman. "The spectral radius of large random matrices." *The Annals of Probability* (1986): 1318-1328.
11. N. Alon, et al. "On the concentration of eigenvalues of random symmetric matrices." *Israel Journal of Mathematics* 131.1 (2002): 259-267.
12. P. Dueck, et al. "Spectral Properties of Large Random Matrices with Independent Entries."


Department of Mathematics, Princeton University
*E-mail address*: petter@princeton.edu